



120
344
THS



3 1293 00917 5526

This is to certify that the
thesis entitled
**Bi and PbO Addition and Liquid
Phase Sintering of 123 Compound**
presented by
Il-Sung Oh
has been accepted towards fulfillment
of the requirements for
Master's degree in Metallurgy


Major professor

Date 5/11/90

LIBRARY
Michigan State
University

PLACE IN RETURN BOX to remove this checkout from your record.
 TO AVOID FINES return on or before date due.

DATE DUE	DATE DUE	DATE DUE
06 1995		

MSU is An Affirmative Action/Equal Opportunity Institution

c:\clic\dtedue.pm3-p.1

**Bi AND PbO ADDITION AND LIQUID PHASE SINTERING
OF Y-Ba-Cu-O COMPOUND**

BY

Ilsung Oh

A THESIS

**Submitted to
Michigan State University
in partial fulfillment of the requirements
for the degree of**

MASTER OF SCIENCE

Department of metallurgy, Mechanics and Material Science

1990

ABSTRACT

Bi AND PbO ADDITION AND LIQUID PHASE SINTERING OF Y-Ba-Cu-O COMPOUND

By

Ilsung Oh

The relatively low sintered density of Y-Ba-Cu-O superconducting compound is the typical of consolidation and sintering of its powdered components. Such a porous structure further degrades mechanical stability of intrinsically brittle Y-Ba-Cu-O compound. A study was conducted to develop an economically attractive processing technique based on liquid phase sintering, which can reduce porosity and upgrade mechanical properties without degrading superconducting properties. Bi and PbO were added in Y-Ba-Cu-O compound to employ liquid phase sintering. The mixture was compacted and sintered at 920 and 950 C. It was observed that addition of PbO reduced porosity by 7 to 8% without affecting transition temperature while addition of Bi did not reduce porosity. It was also found that both of Bi and PbO reacted with 1:2:3 compound to form non-superconducting phases.

In this thesis, the details of sample preparation, experimental results of x-ray analysis, transition temperature and density measurements, optical and scanning electron microscopy and EDAX analysis are presented.

ACKNOWLEDGEMENTS

First of all, I would like to express my deepest thanks to professor Dr. K. Mukherjee and my parents for their constant support and kind guidance during this research. I would like to thank Dr. P.A.A. Khan for his valuable suggestions and comments. I would also like to thank to Mr. G. Jang, J. Yoo and C. Chen for their timely support and help. Finally, I would like to express personal appreciation to my wife Youngah Jung for her continuous encouragement.

TABLE OF CONTENTS

	Page
LIST OF FIGURES	iv
LIST OF TABLES	vi
1. INTRODUCTION	1
2. LITERATURE SURVEY	
2-1 The Effect of Added Impurities on Y-Ba-Cu-O Compound	4
2-2 Some Processing Techniques to Decrease Porosity	10
3. EXPERIMENTAL PROCEDURE	
3-1 Sample Preparation	15
3-2 X-ray Measurements	16
3-3 Transition Temperature Measurements	17
3-4 Density Measurements	22
3-5 Morphological Examination and EDAX Analysis	
3-5-1 Optical Microscopy	24
3-5-2 Scanning Electron Microscopy and EDAX Analysis	24
4. RESULTS AND DISCUSSION	
4-1 X-ray Diffraction Data	25
4-2 Critical Transition Temperature Measurements	30
4-3 Density Measurements	34
4-4 Optical Microscopy	36
4-5 Scanning Electron Microscopy and EDAX Analysis	43
5. SUMMARY	53
6. REFERENCES	54

LIST OF FIGURES

Figure	Page
1. The normalized (at 100 K) resistivity as a function of temperature for 1:2:3 compound doped with Cr Mn, Ti, V, Fe and Zn (Ref 7)	6
2. Superconducting transition temperature, T_c (midpoint), $T_{0.9}$ (90% of the sigmoid) and $T_{0.1}$ (10%) in doped 1:2:3 plotted against the dopant valence (Ref 7)	7
3. T_c (solid line) and magnetic susceptibility at 100 K (dashed line) of 1:2:3 compound doped with 3d element, as a function of the number of valence electrons (Ref 5)	8
4. Resistance curve as a function of temperature for different specimens. E1 correspond to specimen after pressing and E1A correspond to specimen after pressing and postannealing (Ref 11)	12
5. Magnetic susceptibility vs. temperature curve for melt processed 1:2:3 compound (Ref 12)	13
6. Schematic diagram of resistance measurement set-up	18
7. Schematic diagram of four wire AC resistance measurement	19
8. Schematic diagram of sample holder assembly for 4 wire AC resistance measurement	20
9. X-ray diffraction patterns of pure 1:2:3 sample and 1:2:3 mixed with PbO, sintered at 950 C	26
10. X-ray diffraction patterns of pure 1:2:3 sample and 1:2:3 mixed with PbO, sintered at 920 C	27
11. X-ray diffraction patterns of pure 1:2:3 sample and 1:2:3 mixed with Bi, sintered at 950 C	29
12. Temperature effect on resistance of pure 1:2:3 sample and 1:2:3 mixed with Bi or PbO - 1	32
13. Temperature effect on resistance of 1:2:3 samples mixed with Bi or PbO - 2	33

14. Optical microscopy of pure 1:2:3 sample, sintered at 920 C (a) 500x (b) 2000x	37
15. Optical microscopy of PbO 5 wt% mixed sample, sintered at 920 C (a) 500x (b) 2000x	38
16. Optical microscopy of PbO 10 wt% mixed sample, sintered at 920 C (a) 500x (b) 2000x	40
17. Optical microscopy of PbO 15 wt% mixed sample, sintered at 920 C (500x)	41
18. Optical microscopy of Bi mixed samples, sintered at 950 C (500x) (a) Bi 5 wt% (b) Bi 10wt%	42
19. SEM micrographs of (a) pure 1:2:3 sample (b) PbO 5 wt% mixed sample, sintered at 920 C	44
20. SEM micrographs of (a) PbO 10 wt% mixed sample (b) PbO 15 wt% mixed sample, sintered at 920 C	45
21. EDAX spectra obtained from pure 1:2:3 sample, sintered at 920 C	46
22. EDAX spectra obtained from PbO 5 wt% mixed sample, sintered at 920 C	47
23. EDAX spectra obtained from PbO 10 wt% mixed sample, sintered at 920 C	48
24. EDAX spectra obtained from the selected grain marked by arrow in Fig 19b	49
25. EDAX spectra obtained from the selected grain marked by a in Fig 20a	50
26. EDAX spectra obtained from the selected grain marked by b in Fig 20a	51

LIST OF TABLES

Table	Page
1. Various preparation conditions and transition temperatures of pure 1:2:3 samples and 1:2:3 mixed with Bi or PbO	31
2. Measured density and porosity of pure 1:2:3 samples and 1:2:3 mixed with PbO	35

1. INTRODUCTION

Since the discovery of new class of high transition temperature ($T_c = 90$ to 95 K) ceramic superconductor, $YBa_2Cu_3O_{7-x}$ by Wu et al.[1] in 1987, enormous world wide efforts have been made both to enhance the superconducting properties and to develop the practical applications of this new material. Up to now, a large amount of work has been performed to understand the origin of superconductivity and to observe the effect of various element substitution on superconducting properties. It has been found that Y in $YBa_2Cu_3O_{7-x}$ can be replaced by almost all the rare-earth elements without deteriorating T_c [2,3] and the substitution in the Ba site by 25% Sr also does not affect T_c [4]. On the contrary, even small amount of substitution of Cu by 3-d elements degrades the superconducting properties [5,6]. There are several reports that the addition of oxide, nitride, carbonate and some transition metal impurities also affect the superconductivity depending on the types of the reactions between additives and superconducting phase [7,8].

Y-Ba-Cu-O superconductors are known to have some undesirable properties. For instance, the relatively low sintered-density of Y-Ba-Cu-O compound is the typical of consolidation and sintering of powdered components. Such a porous structure further degrades not only the mechanical stability of intrinsically brittle Y-Ba-Cu-O compound for many applications but also the critical current density due

to poor connectivity between individual superconducting grains. Efforts have also been made to remove some of the undesirable characteristics such as high porosity, brittleness, and residual impurity of Y-Ba-Cu-O compound [9,10]. Processing techniques such as HIP (Hot isostatic pressing), hot pressing and melt processing have been tried to improve mechanical properties and critical current density of Y-Ba-Cu-O compound by reducing porosity [11-13].

The purpose of this research is to develop an economically attractive processing technique which can reduce porosity and thereby improve mechanical properties without degrading superconducting properties. The technique is based upon liquid phase sintering, in which different amounts of low melting point additives are mixed in Y-Ba-Cu-O compound. In this research, the effect of Bi and PbO addition in Y-Ba-Cu-O compound on reduction in porosity, the superconducting properties and microstructure was investigated. Bi and PbO were selected as additives to employ liquid phase sintering since they had lower melting points than Y-Ba-Cu-O compound and thus were expected to act as fluxes during the sintering stage.

In this research, X-ray diffraction data was collected to identify phases present in samples. The transition temperature was measured by using a standard four probe technique and the sintered density was measured by using the buoyance method. Optical and scanning electron microscopy were used to examine the morphology of the material. Elemental analysis with an energy dispersive X-ray analyzer

(EDAX) was also carried out to observe the presence of the additives. The details of the experiments and the results of this reserch are discussed in this thesis.

2. LITERATURE SURVEY

2-1 The Effect of Added Impurities On Y-Ba-Cu-O Compound

The effect of the addition of various elements on the superconducting properties of Y-Ba-Cu-O compound was investigated by several researchers to understand its interaction with different additives for the development of practical applications [7,8,14]. The study provided useful information about 1:2:3 processing such as the possibility of contamination from crucibles, possible electric and thermal contact materials, potential densification aids and acceptable contamination levels.

Jarvinen et al. [8] investigated the interaction of 22 different additives with Y-Ba-Cu-O compound; 10 mol% of each impurity (approximately 1 to 4 wt% depending on the molecular weight) was added to Y-Ba-Cu-O powder as oxides or carbonates. According to their results, large number of materials such as ZrO_2 , V_2O_5 , Nb_2O_5 , WO_3 , Bi_2O_3 , In_2O_3 , SiO_2 , TiO_2 , BaO , and Sb_2O_5 have been shown to produce only a small change in resistance vs. temperature behavior and indicate a similar X-ray diffraction pattern of the orthorhombic phase as compared to that of pure Y-Ba-Cu-O compound. On the contrary, several materials such as Co_2O_3 , MoO_3 , Fe_2O_3 , and Al_2O_3 were found to totally destroy the orthorhombic superconducting phase and transform it to tetragonal phase.

The effect of transition-metal impurities on the superconducting properties of Y-Ba-Cu-O compound was reported by Dou et al. [7]. Samples with the composition of $\text{YBa}_2\text{Cu}_3\text{M}_z\text{O}_{7-x}$ were fabricated by adding transition metal oxides in the Y-Ba-Cu-O powders (where $\text{M} = \text{Fe}, \text{Ni}, \text{Zn}, \text{Sc}, \text{Ti}, \text{V}, \text{Cr}, \text{Mn}$ and $z = 0.06$). Fig 1 shows the temperature dependence of the normalized resistance for these samples. It can be seen that samples with Fe and Zn drops T_c sharply and have semiconductor-like temperature-resistivity behavior with a negative temperature derivative of resistivity whereas other samples have metal-like behavior. It is also noted that the non-magnetic Zn degrades T_c more strongly than magnetic Fe. For the reduction of T_c by transition metal other than Fe and Zn, they proposed that it depends on the oxidation potential of these cations; i.e. dopant element with higher oxidation state reduce T_c less than that with a lower oxidation state. Fig 2 shows T_c values against valencies for V^{5+} , Ti^{4+} , Mn^{4+} , Cr^{3+} and Ni^{2+} .

The similar phenomenon was observed by Xiao et al. [5] who studied the effect of 3-d element substitution for Cu in Y-Ba-Cu-O compound. They suggested that T_c is strongly correlated with the size of paramagnetic moments of doped elements and T_c suppression arises from the breakage of conducting Cooper-pairs by d-electron scattering at the paramagnetic site. Fig 3 shows the values of T_c and susceptibility at $T = 100 \text{ K}$ for the different 3-d elements. It can be seen that the large paramagnetic moment of Fe

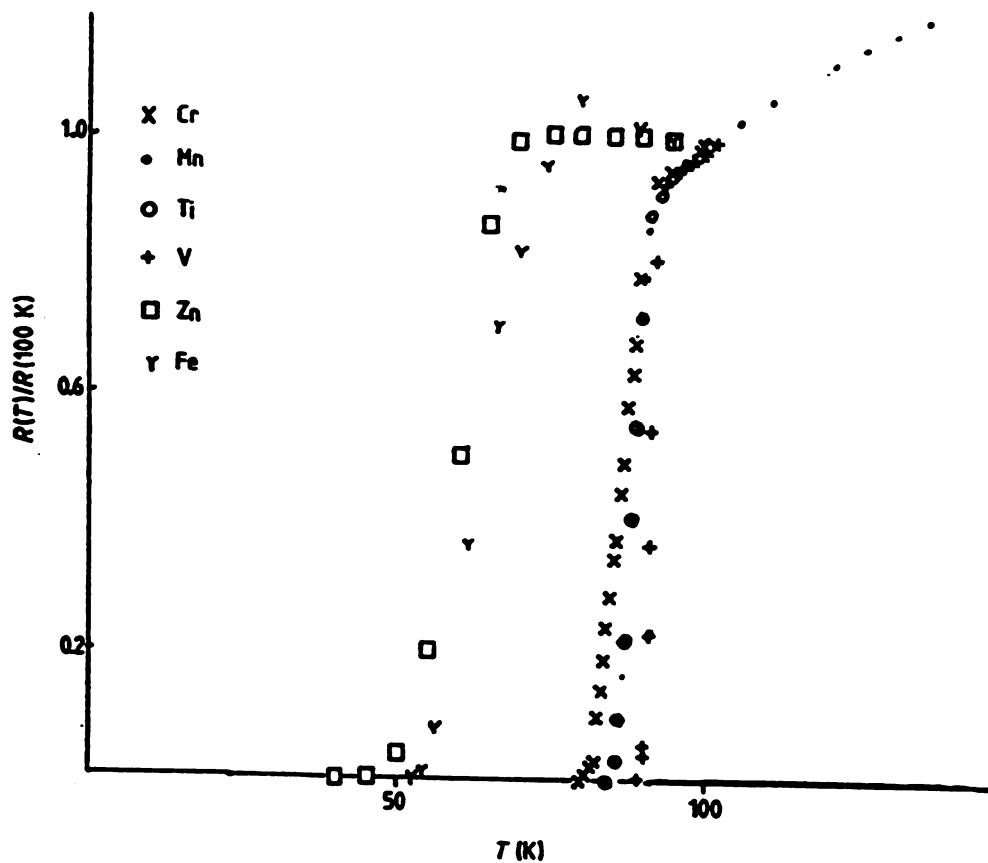


Fig. 1. The normalized (at 100 K) resistivity as a function of temperature for 1:2:3 compound doped with Cr, Mn, Ti, V, Fe and Zn (Ref 7).

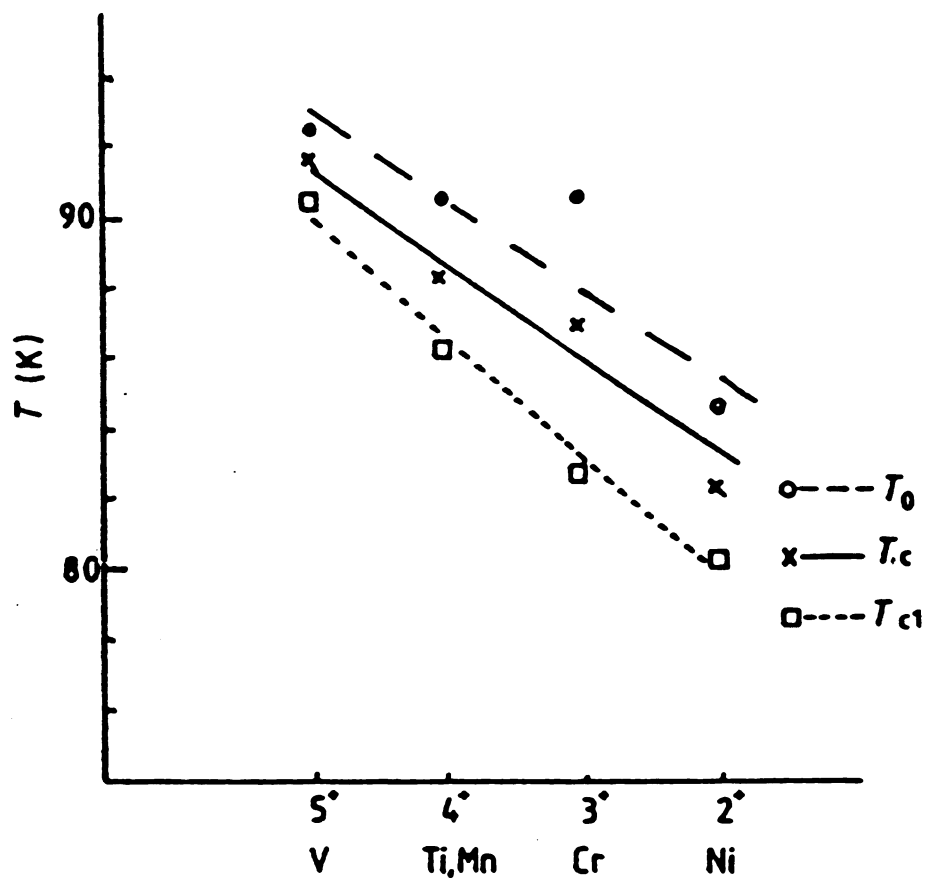


Fig. 2. Superconducting transition temperature, T_c (midpoint), T_0 (90% of the sigmoid) and T_{c1} (10%) in doped 1:2:3 plotted against the dopant valence (Ref 7).

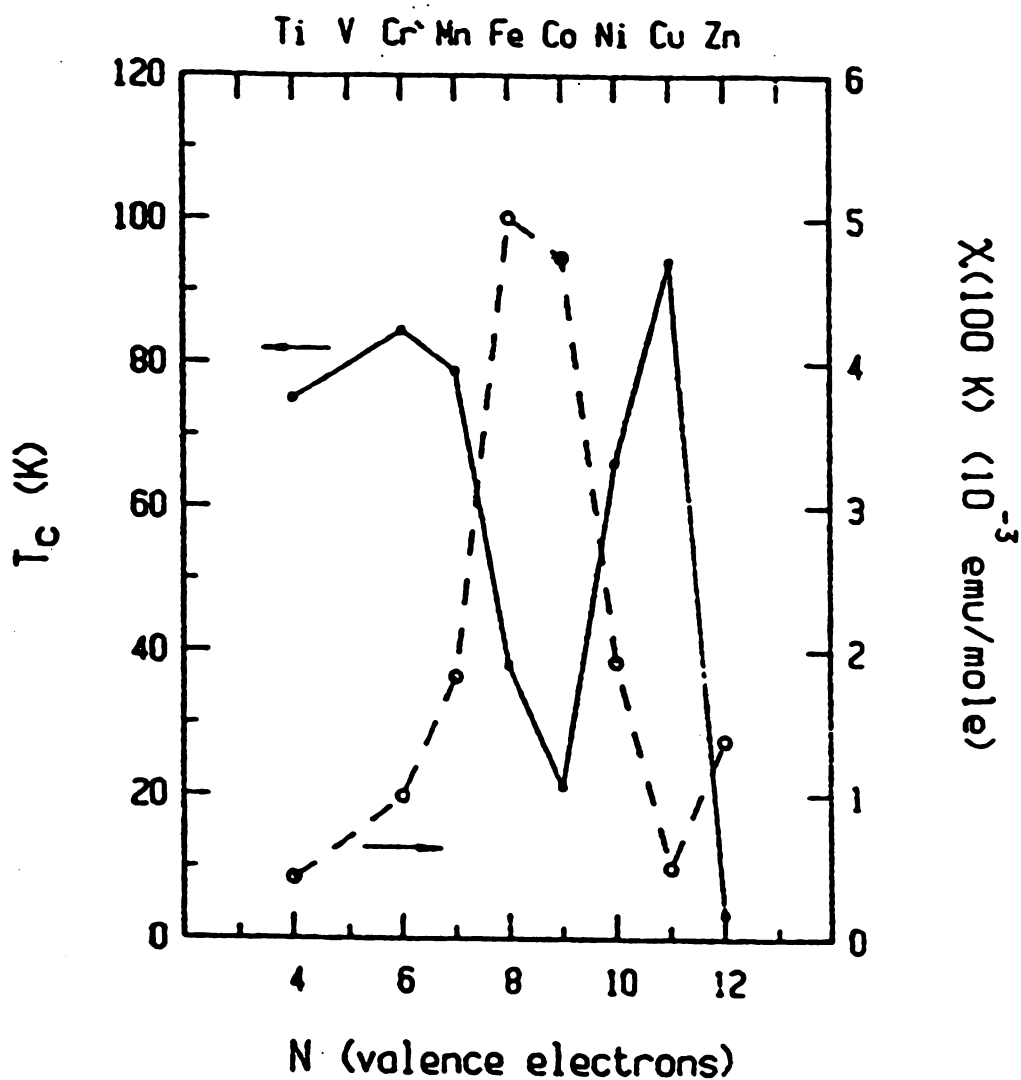


Fig. 3. T_c (solid line) and magnetic susceptibility at 100 K (dashed line) of 1:2:3 compound doped with 3d element, as a function of the number of valence electrons (Ref 5).

degrades T_c more strongly than other elements. For the non-magnetic Zn which has the stronger influence on T_c than Fe, they explained the T_c reduction in terms of the filled 3-d shell of Zn; i.e. the substitution of Cu by Zn provide an extra electron for the divalent Cu shell (9 electrons), which fill up the antibonding d-band and reduce the density of state at the Fermi-level.

On the contrary, other authors [6,15] proposed that T_c reduction is not necessarily of magnetic origin. For instance, Maeo et al. [6] suggested that the valencies of the doped ion or properties related to the valency such as differences in ionic radii are more important in determining the impurity effect. However, a clear explanation is not yet available.

Addition of Ag in Y-Ba-Cu-O compound drew special interests of many researchers since it had been shown to enhance the critical current density and mechanical characteristics while leaving other superconducting properties unchanged [16-18]. Pavuna et al. [17] reported that superconductivity of Y-Ba-Cu-O compound is preserved even up to 50 wt% of silver addition and the magnitude of electrical resistivity at 300 K rapidly decreases as the amount of silver increases. Ag addition was also found to have an effect on decreasing porosity, improving critical current density, and reducing the contact resistance [18].

2-2 Some Processing Techniques to Decrease Porosity

It has been found that it is difficult to obtain high density of polycrystalline Y-Ba-Cu-O compound by solid state sintering since sintering temperature is limited by phase stability and incipient melting considerations. Kumahura et al. [19] reported that although a drastic reduction in porosity in Y-Ba-Cu-O compound occurred when heat treated above 1030 C due to partial melting of the sample, high temperature heat treatment caused the formation of a large amount of non-superconducting phases in addition to $\text{YBa}_2\text{Cu}_3\text{O}_{7-x}$, and consequently degraded the critical current density due to weak coupling between the superconducting grains. Thus, several processing techniques have been applied to make highly dense bulk Y-Ba-Cu-O compound and thereby enhance mechanical characteristics and critical current density.

HIP (hot isostatic pressing) densifies powder particles by massive movement of material through hot deformation instead of the diffusion of individual atoms as in sintering. Consequently, rapid densification can be obtained at relatively lower temperature and shorter times than in sintering. Tien et al. [20] reported that fully dense Y-Ba-Cu-O compound can be obtained with many combinations of pressure, temperature and time during HIP, and furthermore the electrical and mechanical properties of the superconductor can be improved by controlling the mechanisms of powder deformation during HIP which allow the

densification to take place through a chosen deformation process.

The effect of hot isostatic pressing on transition temperature of Y-Ba-Cu-O compound was investigated by Sadananda et al. [11]. Fig 4 shows temperature dependence of resistance before and after post-annealing for the pressed samples. It can be seen that subsequent pressing, although it compacted the sample to almost theoretical density, reduced T_c to 65 K as compared to 92 K after initial sintering and annealing in the non-pressed sample. They suggested that T_c reduction for the pressed sample resulted from either some oxygen loss during encapsulation of sample in vacuum or partial disorder occurred during heating, and consequently appropriate post-annealing is necessary to recover this T_c reduction.

Fabrication of Y-Ba-Cu-O superconductor by an oxide melting method in place of conventional sintering was also attempted by several authors [12,21,22]. Jin et al. [12] reported that melt processing such as melt drawing or melt spinning could be a convenient fabrication method for obtaining superconducting wires or ribbons with greatly improved density and electrical properties. Fig 5 is magnetic susceptibility vs. temperature curve which shows the effect of melt processing on transition temperature. It can be seen that while as-sintered and solidified sample is non-superconducting, superconductivity is fully recovered after a homogenization heat treatment followed by

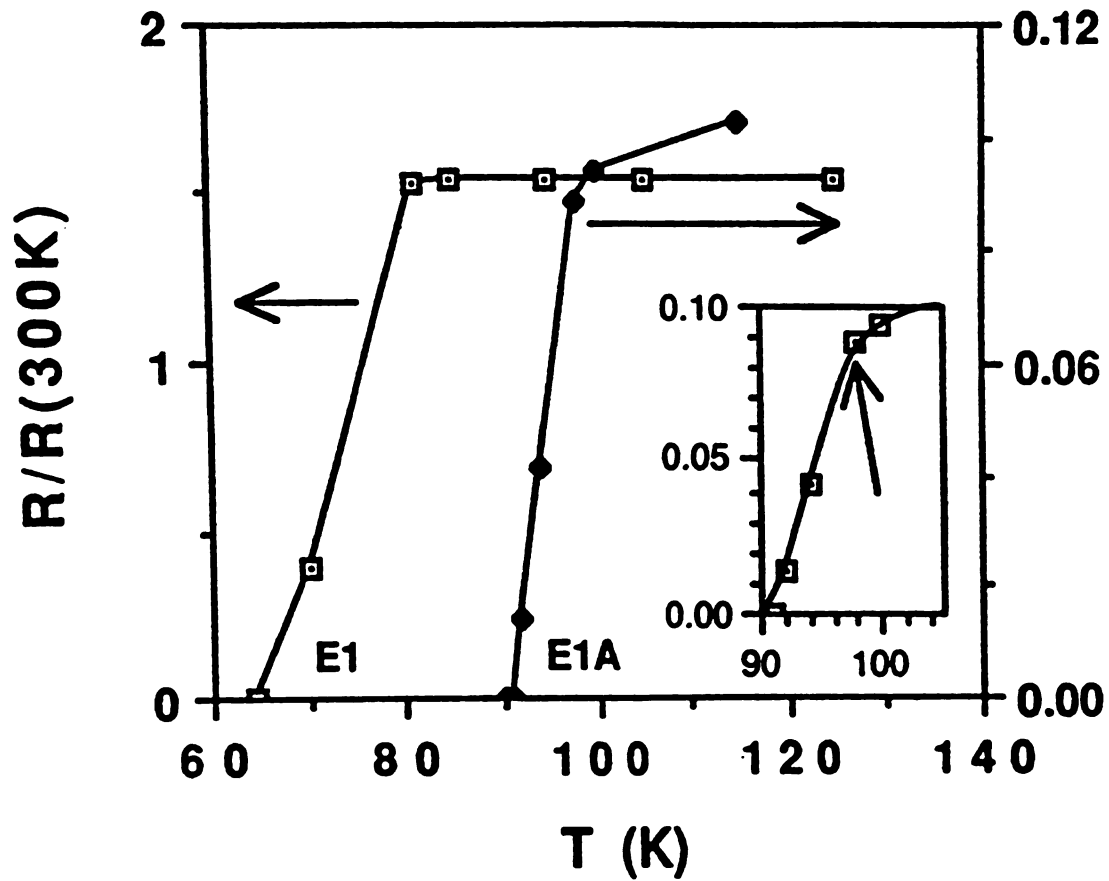


Fig. 4. Resistance curve as a function of temperature for different specimens. E1 correspond to specimen after pressing and E1A correspond to specimen after pressing and postannealing (Ref 11).

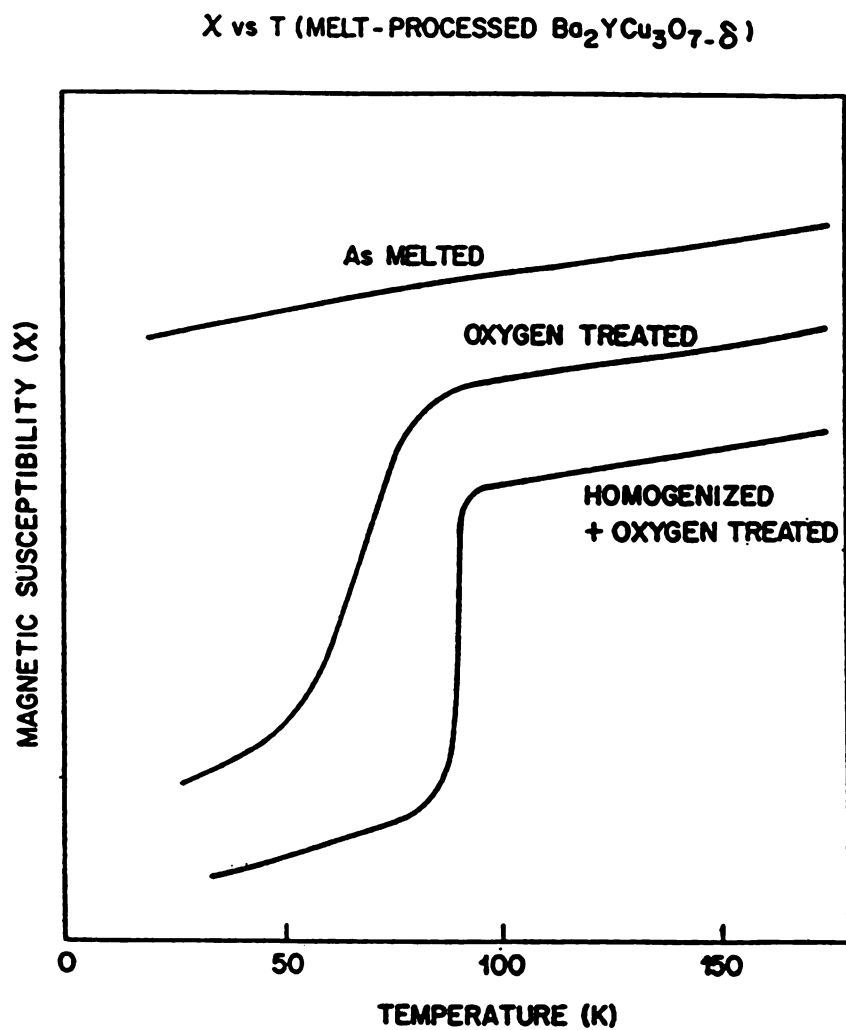


Fig. 5. Magnetic susceptibility vs. temperature curve for melt processed 1:2:3 compound (Ref 12).

oxygen heat treatment. Therefore, special post heat treatment is essential in melt processing for recovering superconductivity which disappears during high temperature process.

It was also reported [22] that melt-textured growth of Y-Ba-Cu-O compound from a supercooled melt produced an nearly 100% dense structure consisting of locally aligned, long, needle-shaped grains, and this new structure has a sharply higher critical current density than the conventionally sintered materials and furthermore much reduced field dependence of critical current density. It was suggested that the increase in critical current density for the melt processed sample can be explained by three combined factors such as (1) the formation of dense structure, (2) grains alligned parallel to the a-b conduction band in this anisotropically conductive layered compound and (3) the formation of cleaner grain boundary area.

3. EXPERIMENTAL PROCEDURE

3-1 Sample Preparation

$\text{YBa}_2\text{Cu}_3\text{O}_{7-x}$ powder was prepared from high purity (99.99%) of Y_2O_3 , BaCO_3 and CuO powders. These powders were weighed on a calibrated micro balance and mixed to have Y:Ba:Cu cation ratio of 1:2:3. The powder mixed with methanol was thoroughly ground with a pestle and mortar to ensure complete mixing. The mixed powder was then dried in air to evaporate the methanol. The dried powder was placed in an alumina crucible and calcined at 930 C (1203 K) in air atmosphere for 24 hours. The calcined powder was slowly cooled down to room temperature inside the furnace.

The $\text{YBa}_2\text{Cu}_3\text{O}_{7-x}$ powder was again regrounded with a pestle and mortar. In regrounded $\text{YBa}_2\text{Cu}_3\text{O}_{7-x}$ powder, various amounts of Bi (99.99% pure) or PbO (99.9% pure) powders were added to obtain $(\text{YBa}_2\text{Cu}_3\text{O}_{7-x})_{1-y}\text{A}_y$, where A = Bi and PbO, y = 5 wt% and 10 wt% for Bi and 5 wt%, 10 wt% and 15 wt% for PbO. The mixtures were uniaxially pressed into one inch diameter pellets under a pressure of 10,000 psi and then sintered for 12 hours at two different temperatures of 920 C (1193 K) and 950 C (1223 K) in air atmosphere. The sintered pellets were slowly cooled down to room temperature inside the furnace. For comparison, the parent sample of $\text{YBa}_2\text{Cu}_3\text{O}_{7-x}$ unmixed with Bi or PbO was also made under similar processing conditions.

3-2 X-ray Measurements

For the structural analysis and phase identification, X-ray diffraction experiment was carried out. X-ray diffraction data was obtained by using Ni-filtered Cu-K α radiation with a Scintac XDS 2000 diffractometer. A tube voltage of 36 kV and tube current of 25 mA was used for these measurements. As-sintered surface was used for this purpose.

3-3 Transition Temperature Measurements

A continuous measurement of resistance as a function of temperature was carried out by means of an auto balancing AC bridge with a lock-in amplifier using a standard four-probe technique. Fig 6 shows the schematic diagram of electrical resistance measurement set-up. A LR-400, four wire AC resistance bridge and a Houston instrument 200, X-Y recorder were used for these measurements. Liquid nitrogen was used for cooling the sample.

Fig 7 shows a schematic of the four wire AC resistance measurement system. In this diagram, four gold-plated pins were attached to the test sample. The two outer ones were for current supply and the inner two were for voltage measurement.

A copper-constantan thermocouple was attached to the center of the specimen. This kind of bimetallic joint produces small electrical voltage and the exact value of this small voltage varies with the temperature of the area around the thermocouple junction. Therefore, temperature was determined by converting this voltage to temperature by using conversion table [23]. Contacts were made by inserting the superconductor pellet and gold-plated pins between two PVC blocks as was seen in Fig 8. All were then clamped with two plastic clamps and were immersed in the liquid nitrogen reservoir for cooling.

The electrical resistance was monitored by the LR-400 AC resistance bridge in the temperature range from room

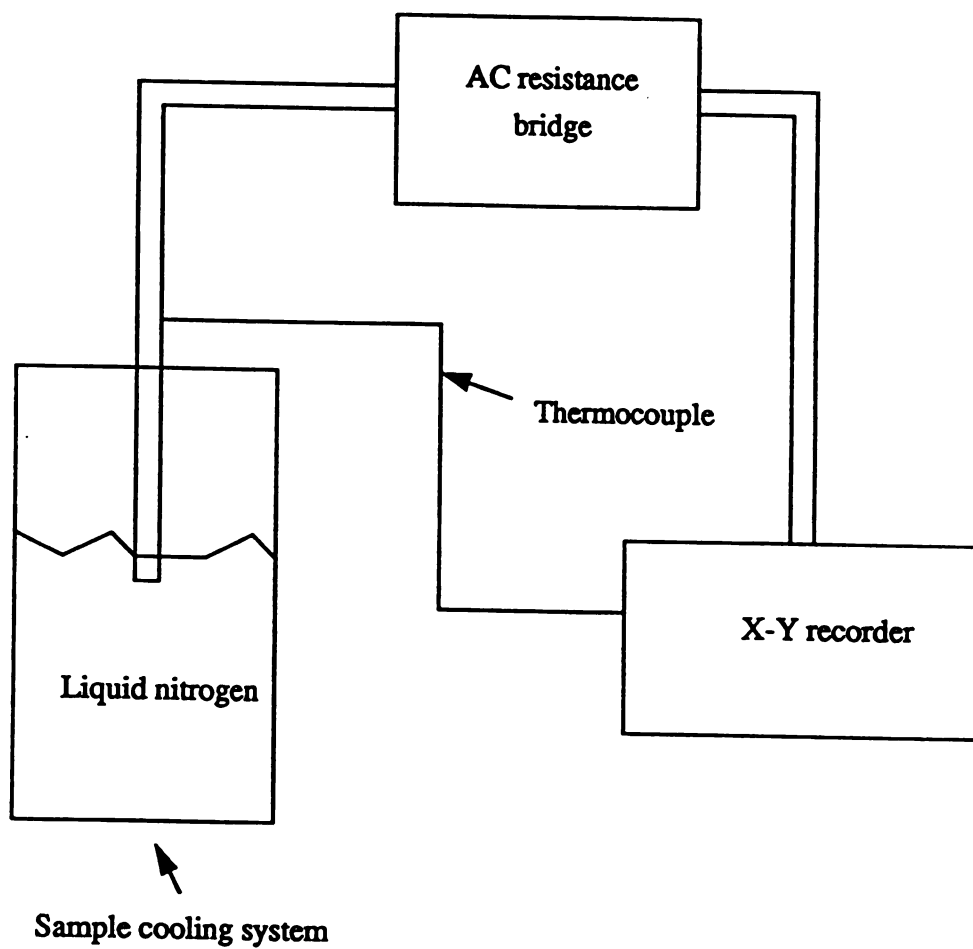


Fig. 6. Schematic diagram of resistance measurement set-up.

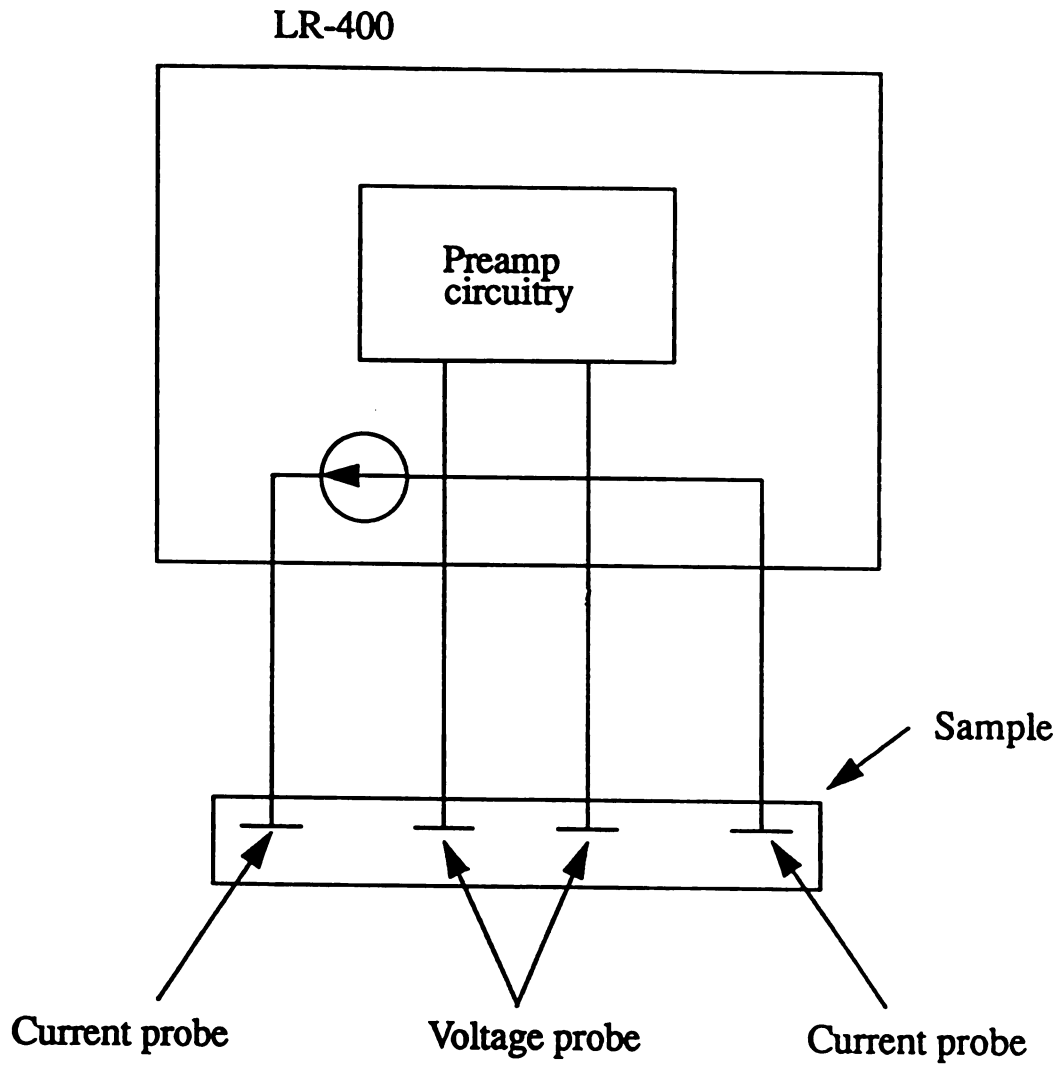


Fig. 7. Schematic diagram of four wire AC resistance measurement.

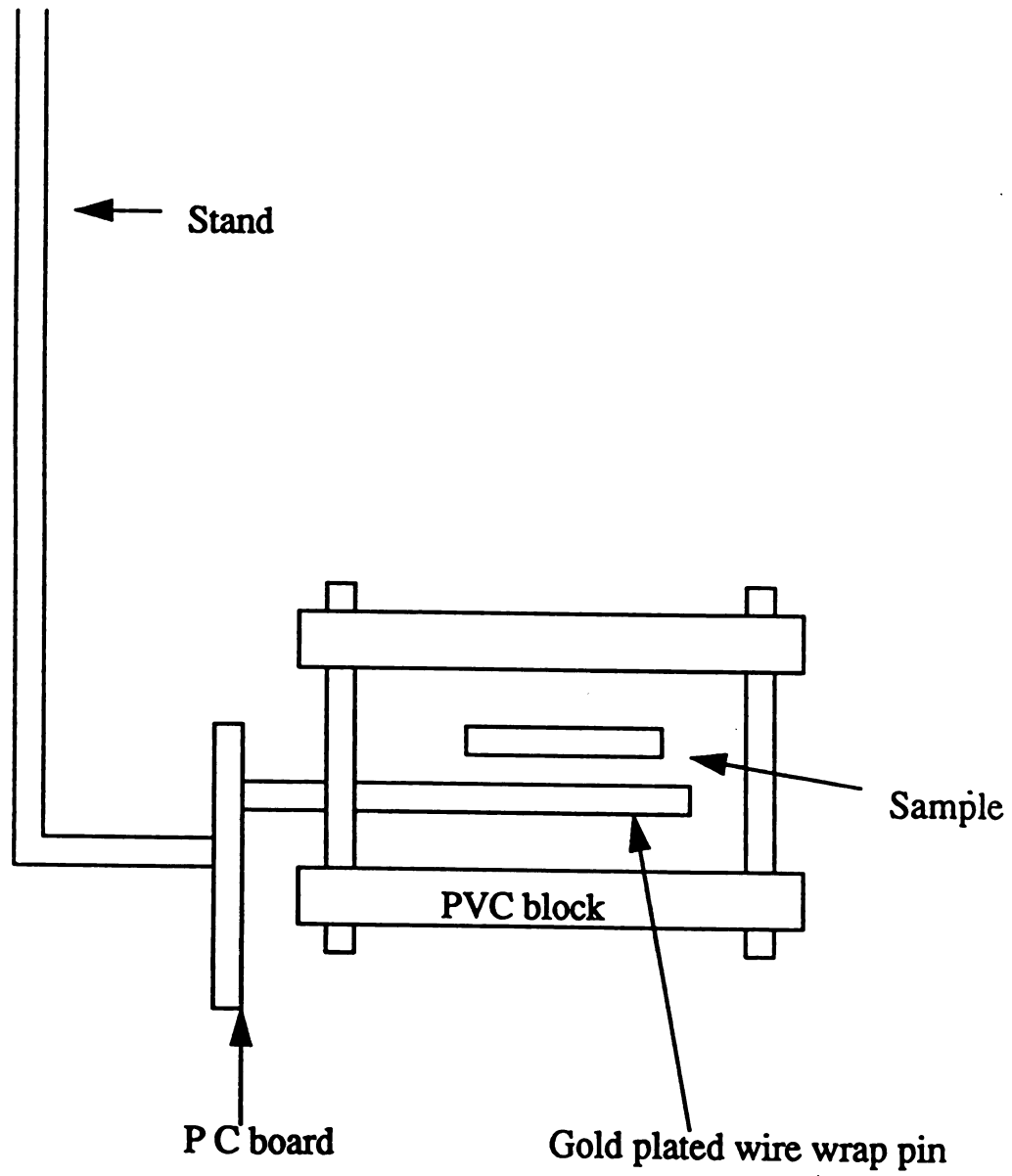


Fig. 8. Schematic diagram of sample holder assembly for 4 wire AC resistance measurement.

temperature to liquid nitrogen temperature (77 K). The resolution of the machine was 1 micro-ohm and an excitation current of 3 mili ampere was used for these measurements.

3-4 Density Measurements

The density of sintered samples was measured by using the buoyancy method following ASTM B 328-73 [24]. First, samples were cleaned with acetone and methanol and then completely dried in air. After obtaining the dry weights of the samples (weight, W_a), they were immersed in SAE 10W-40 motor oil (viscosity of approximately 200 SUS at 100 F), held for 6 hours at 182 C and then cooled to room temperature by immersion in oil at room temperature. This procedure allows the oil to be impregnated through interconnected pores of the sintered samples.

After weighing oil impregnated samples (weight, W_b), they were tied with a fine wire (0.09 mm in diameter) and suspended from the beam hook of the balance. A distilled water filled beaker and bridge was placed underneath the beam hook and sample was completely immersed in the water. The water covered the sample by at least a quarter inch (6.4 mm). Care was taken to ensure that no air bubbles adhere to the sample and the wire. The wired sample was weighed (weight, W_c) and then wire without sample was immersed in water again to the same point as before, and was reweighed (weight, W_e).

The density of the sample was calculated by the following equation;

$$D = \frac{A}{B - C + E}$$

where:

D = density, g/cm^3 ,

A = weight in air of oil-free specimen, g,

B = weight of oil-impregnated specimen, g,

C = weight of oil-impregnated specimen and wire in water,
g, and

E = weight of wire in water, g.

3-5 Morphological Examination and EDAX Analysis

3-5-1 Optical Microscopy

The microstructure was observed on the polished surface of the sintered samples. Samples were mounted in lucite, mechanically ground with abrasive grit papers of 240 to 600 grit and 600 grade emery paper and then polished on a cloth using alumina powder and diamond powder of the size from 2 to 0.5 micrometer. Methanol was used instead of water in order to prevent possible degradation of the superconductor samples due to moisture. Photographs were taken at the magnification of 500 and 2000X using Leco Neophot 21.

3-5-2 Scanning Electron Microscopy and EDAX Analysis

A Hitachi S-2500C SEM with Link energy dispersive x-ray spectroscopy was used to observe microstructure and presence of the additives in the samples. For this purpose, fractured section of specimens were mounted on cylindrical aluminum stubs and silver paint was used for electrical contact to ground.

4. RESULTS AND DISCUSSION

4-1 X-ray Diffraction Data

Fig 9 shows x-ray diffraction patterns for the reference pure 1:2:3 compound and 1:2:3 mixed with PbO sintered at 950 C. It can be seen that PbO 5 wt% mixed sample shows almost identical x-ray pattern to the reference pure 1:2:3 sample. However, some additional peaks (the strongest one at around 30 degree) were found in samples with more than 10 wt% of PbO. The intensity of these additional peaks increases whereas the intensity of peaks from orthorhombic superconducting phase decreases as the amount of PbO increases from 5 to 15 wt%. These additional peaks are considered to come from non-superconducting phases which might result from the reaction between 1:2:3 compound and PbO since they are not coincident with the x-ray diffraction pattern of pure PbO. This was confirmed by observing Meissner effect; samples with more than 10 wt% of PbO showed a weak Meissner effect as compared to that of reference pure 1:2:3 sample, which suggests that these samples contain a considerable amount of non-superconducting phases.

A similar behavior was observed in PbO mixed samples sintered at a lower temperature of 920 C as can be seen in Fig 10. Once again, PbO 5 wt% mixed sample shows almost identical x-ray pattern to the reference pure 1:2:3 sample. However, in the case of samples with more than 10 wt% PbO,

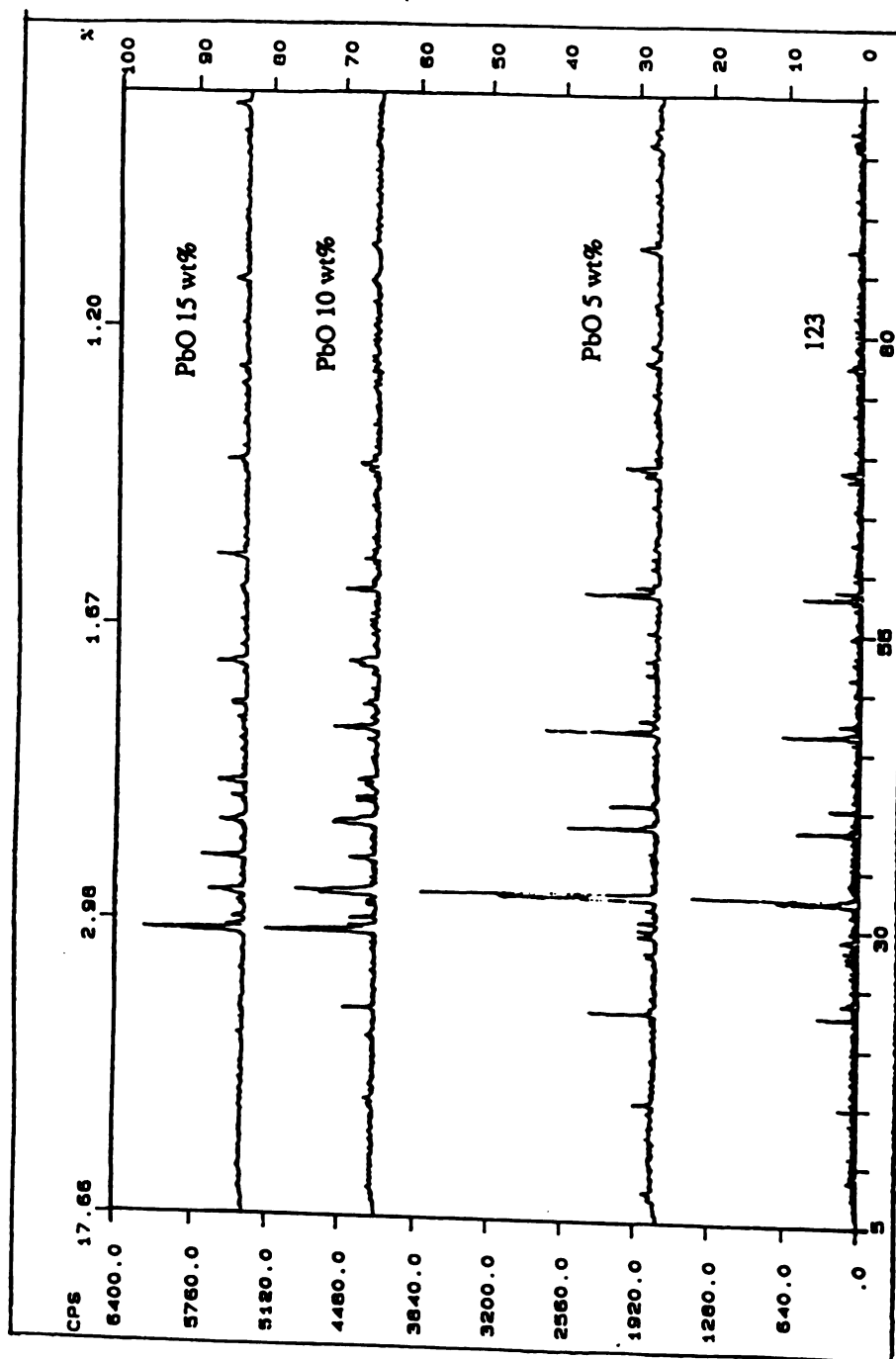


Fig. 9. X-ray diffraction patterns of pure 1:2:3 sample and 1:2:3 mixed with PbO, sintered at 950 C.

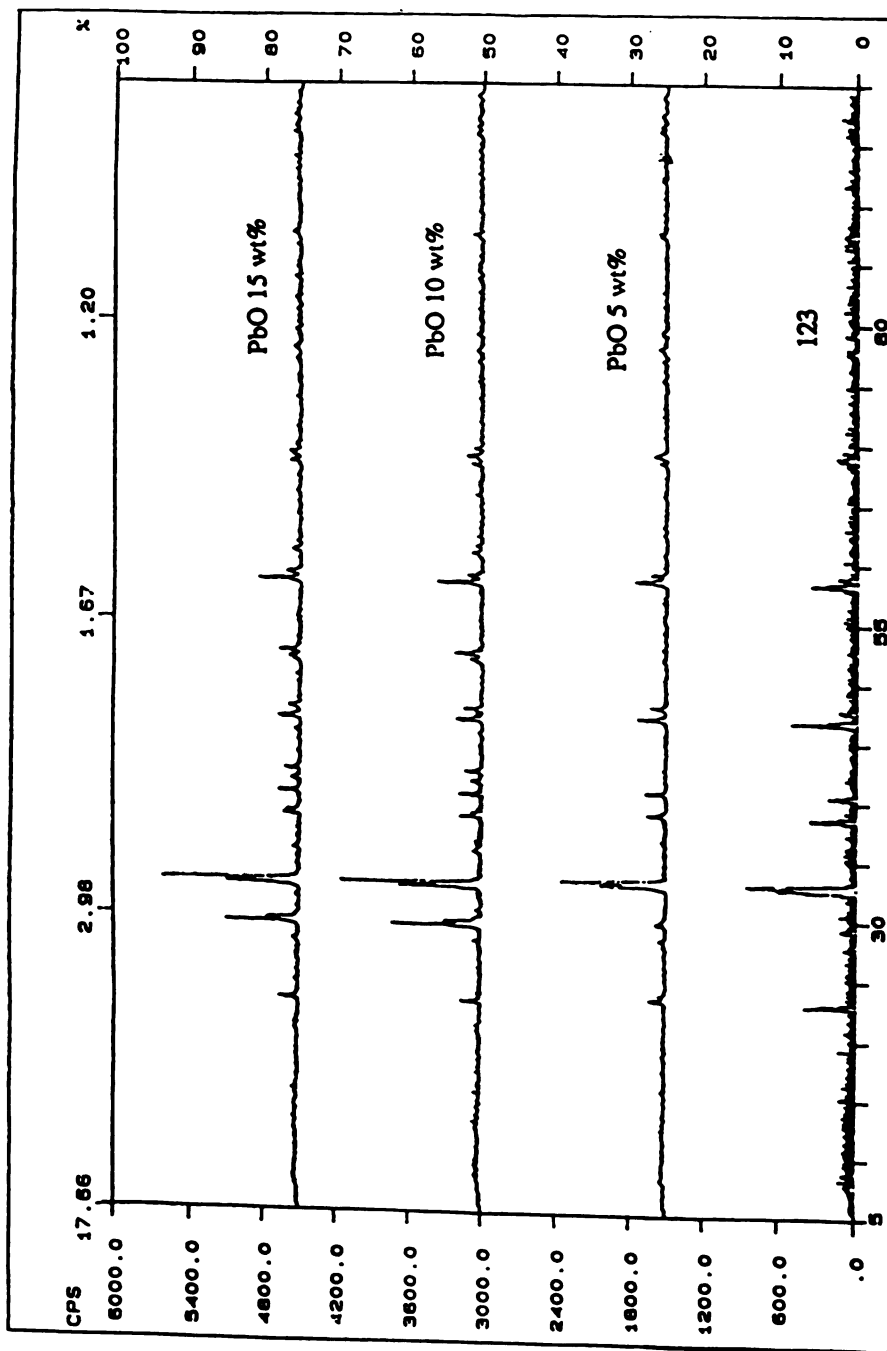


Fig. 10. X-ray diffraction patterns of pure 1:2:3 sample and 1:2:3 mixed with PbO, sintered at 920 C.

the intensity of additional peaks from non-superconducting phase was decreased as compared to that of samples sintered at 950 C. Therefore, it can be assumed that the reaction between 1:2:3 compound and PbO is more active at 950 C than at 920 C.

Fig 11 shows x-ray diffraction patterns for pure 1:2:3 sample and 1:2:3 mixed with Bi sintered at 950 C. It can be seen that even 5 wt% Bi mixed sample shows strong additional peaks from non-superconducting phases. Therefore, data on low temperature sintering, i.e. 920 C is not discussed here.

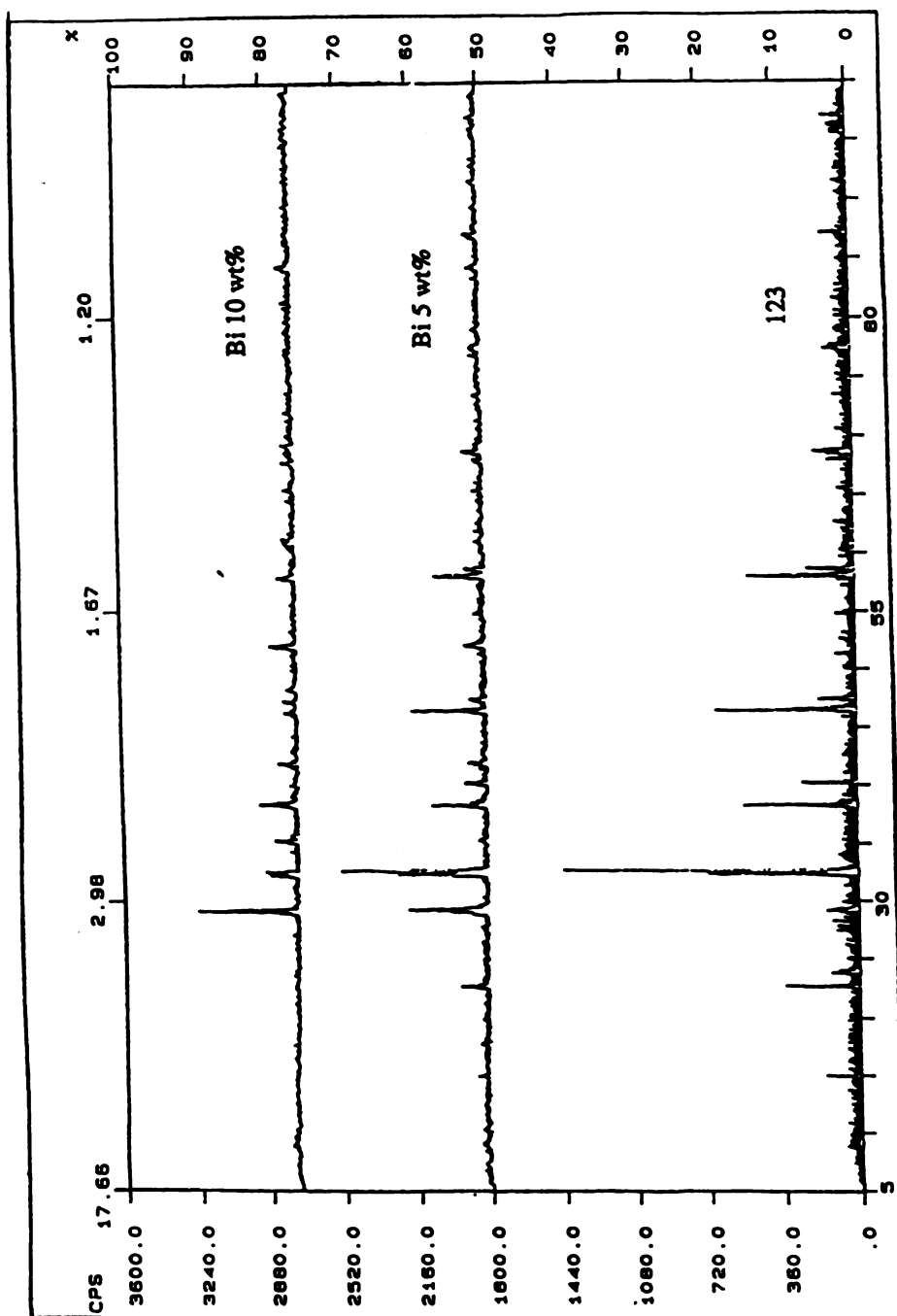


Fig. 11. X-ray diffraction patterns of pure 1:2:3 sample and 1:2:3 mixed with Bi, sintered at 950 C.

4-2 Critical Transition Temperature Measurements

Table 1 shows various preparation conditions and transition temperatures of the reference pure 1:2:3 and 1:2:3 samples with various amounts of Bi or PbO additives. It can be seen that all the samples have transition temperatures between 87 and 92 K and a transition width of 4 to 5 K. These measurements are coincident with the transition temperatures of 90 to 95 K for conventional 1:2:3 materials as reported by other researchers [1,5]. Although a considerable amount of non-superconducting phases was observed in samples with Bi or over 10 wt% PbO as seen in x-ray diffraction data, these phases do not significantly affect the transition temperature. However, it is expected that presence of non-superconducting phases may degrade bulk superconductivity such as critical current density and Meissner effect.

The electrical resistance as a function of temperature for reference pure 1:2:3 samples and samples with Bi or PbO sintered at 950 and 920 C are shown in Fig 12 and Fig 13. It can be seen that all the samples show metallic behavior with a positive temperature derivative of resistance. Furthermore, it can be seen that the room temperature resistance increases with the amount of additives and the sintering temperature. The increase in room temperature resistance can be due to an increase of the amount of non-superconducting phases which resulted from the reaction between 1:2:3 compound and additives.

Table 1

Various preparation conditions and transition temperatures of pure 1:2:3 samples and 1:2:3 mixed with Bi or PbO.

Sample name	Calcining	Sintering	T _{off}	T _{on}	$\Delta T = T_{on} - T_{off}$
123 sample 1	1203 K, air, 24 hrs.	1223 K, air, 12 hrs.	92 K	96 K	4 K
123 sample 2	1203 K, air, 24 hrs.	1193 K, air, 12 hrs.	92 K	96 K	4 K
Bimix-1 (5 wt%)	1203 K, air, 24 hrs.	1223 K, air, 12 hrs.	91 K	96 K	5 K
Bimix-2 (10 wt%)	1203 K, air, 24 hrs.	1223 K, air, 12 hrs.	87 K	92 K	5 K
Pbmix-1 (5 wt%)	1203 K, air, 24 hrs.	1223 K, air, 12 hrs.	88 K	92 K	4 K
Pbmix-2 (10 wt%)	1203 K, air, 24 hrs.	1223 K, air, 12 hrs.	89 K	94 K	5 K
Pbmix-3 (15 wt%)	1203 K, air, 24 hrs.	1223 K, air, 12 hrs.	88 K	93 K	5 K
Pbmix-4 (5 wt%)	1203 K, air, 24 hrs.	1193 K, air, 12 hrs.	92 K	96 K	4 K
Pbmix-5 (10 wt%)	1203 K, air, 24 hrs.	1193 K, air, 12 hrs.	91 K	96 K	5 K
Pbmix-6 (15 wt%)	1203 K, air, 24 hrs.	1193 K, air, 12 hrs.	88 K	93 K	5 K

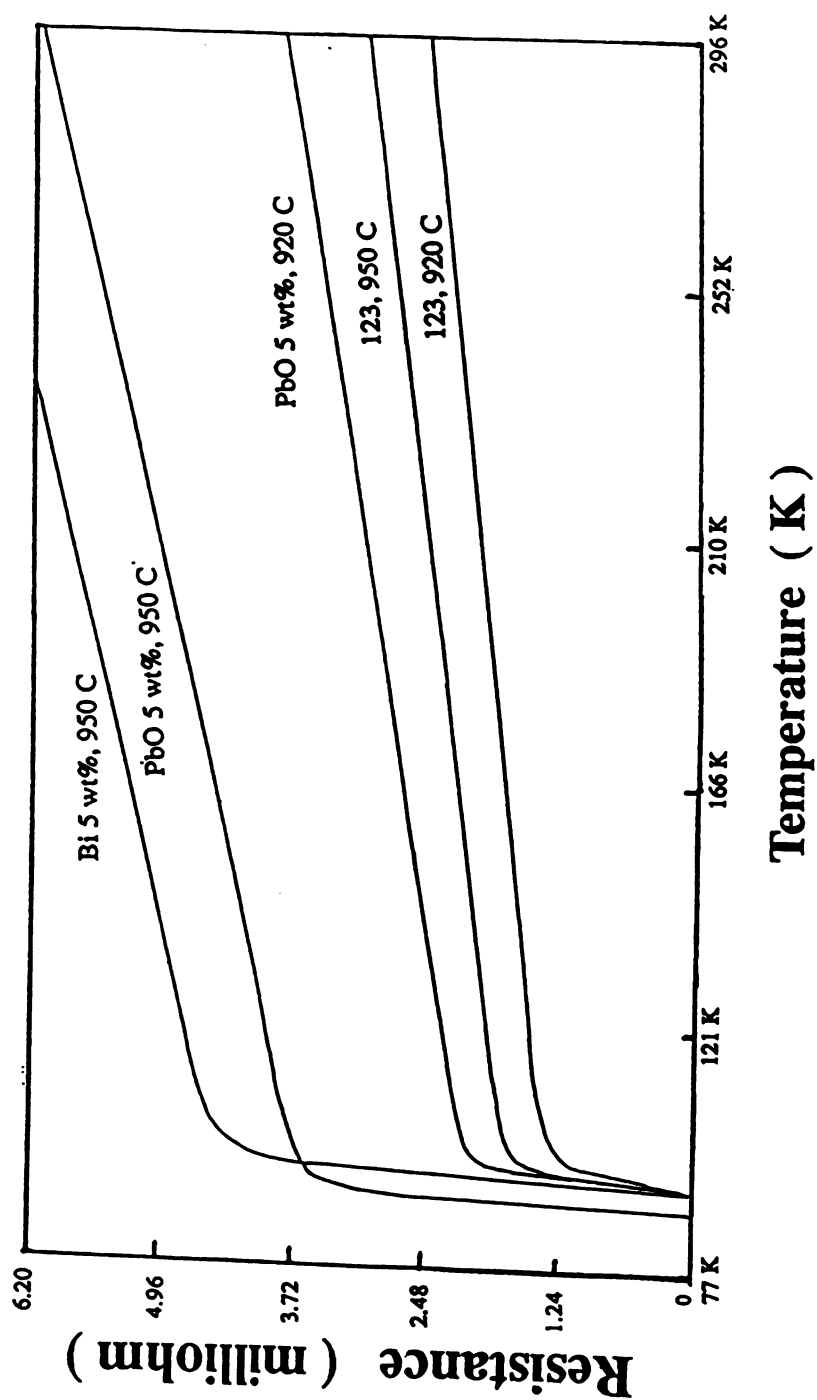


Fig. 12. Temperature effect on resistance of pure 1:2:3 samples and 1:2:3 mixed with Bi or PbO - 1.

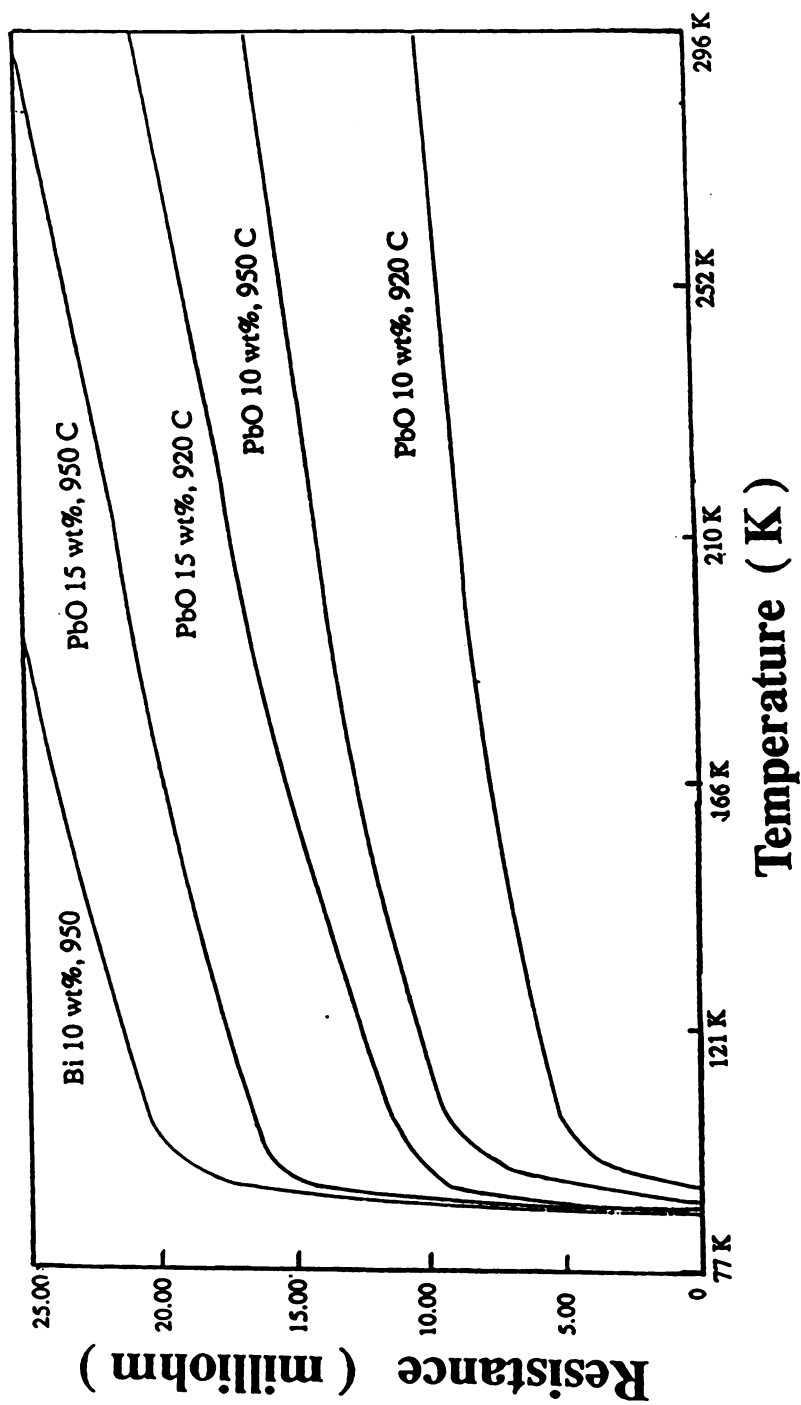


Fig. 13. Temperature effect on resistance of 1:2:3 samples mixed with Bi or PbO - 2.

4-3 Density Measurements

Table 2 shows the measured density and porosity of reference pure 1:2:3 and PbO mixed samples. The porosity was calculated from the ratio between the apparent and theoretical densities. A theoretical density of 6.375 g/cm³ was adopted for YBa₂Cu₃O_{7-x} where x = 0 [25]. The theoretical density of 1:2:3 mixed with PbO was calculated by using the law of mixture. Density of Bi mixed samples was not measured since x-ray data showed that even 5 wt% of Bi addition produces significant amounts of non-superconducting phases, which suggests that Bi is not a suitable element to aid in sintering.

The measured porosity of about 16 to 19% for reference 1:2:3 samples are coincident with the values (15 to 20%) for 1:2:3 sintered conventionally, without any precursor powder preparation technique such as ball milling and pulverizing [18,26]. As can be seen in the table, porosity was improved by about 7 to 8% by the addition of 5 wt% PbO as compared to that of reference pure 1:2:3 samples. The measured value of about 10% porosity for PbO 5 wt% mixed samples is comparable to 7% for sintering-aid doped 1:2:3 compound reported by Patel et al. [26]. However, a further reduction in porosity was not observed in other samples in spite of the increase of PbO addition.

Table 2

Measured density and porosity of pure 1:2:3 samples and 1:2:3 mixed with PbO.

Sample name	Sintering	Wa	Wb	Wc	We	D _{th}	Density	Porosity
123 sample 2	1193 K	3.8590	3.9575	3.2220	0.0125	6.3750	5.1591	19.1
Pb mix-4 (5 wt%)	1193 K	3.1420	3.1660	2.6305	0.0133	6.4823	5.7252	11.7
Pb mix-5 (10 wt%)	1193 K	3.0285	3.0620	2.5546	0.0111	6.5933	5.8409	11.4
Pb mix-6 (15 wt%)	1193 K	2.4235	2.4470	2.0647	0.0102	6.7081	6.0211	10.2
123 sample 1	1223 K	3.7204	3.9045	3.2175	0.0116	6.3750	5.3255	16.5
Pb mix-1 (5 wt%)	1223 K	3.2336	3.2625	2.7230	0.0125	6.4823	5.8580	9.6
Pb mix-2 (10 wt%)	1223 K	3.6795	3.7088	3.0899	0.0125	6.5933	5.8275	11.6
Pb mix-3 (15 wt%)	1223 K	4.0160	4.0263	3.3710	0.0123	6.7081	6.0156	10.3

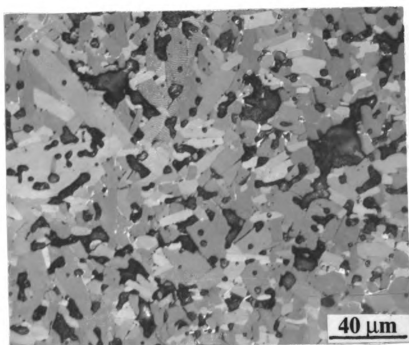
Wa, Wb, Wc, We in grams. Porosity in %

D_{th}: theoretical density of mixture [g / cm³]

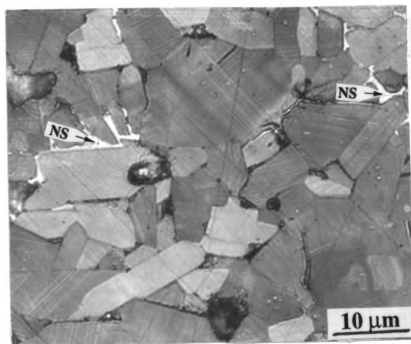
4-4 Optical Microscopy

Fig 14 shows the optical micrograph for reference pure 1:2:3 sample sintered at 920 C. A significant amount of pores can be seen in Fig 14a. The micrograph taken at higher magnification (Fig 14b) shows plate-like grain structure and superconducting grains which contain well formed twin bands resulting from high temperature tetragonal to orthorhombic phase transition [27]. In addition to this superconducting phase, a small amount of non-superconducting phase (marked by NS in Fig 14b) was also observed between some grains, which resulted from off-stoichiometry introduced during mixing process. This non-superconducting phase does not contain twin bands inside the grains.

The optical micrograph for 1:2:3 sample mixed with 5 wt% PbO presented in Fig 15 shows similar structure as pure 1:2:3 except for the reduction in porosity and somewhat increased grain size. However, it can be seen in Fig 15b that the amount of non-superconducting phase was increased as compared to pure 1:2:3 sample. This might have resulted from either off-stoichiometry or reaction between PbO and superconducting 1:2:3 phase. Therefore, it can be assumed that while the formation of these non-superconducting phase decreases the porosity by filling pores, it can affect the critical current density by separating superconducting grains.

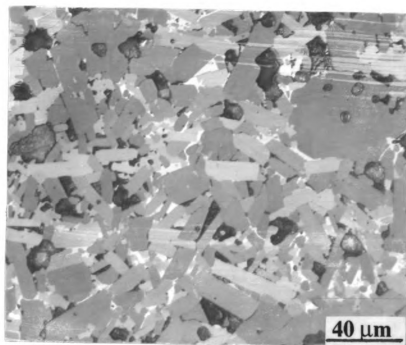


(a)

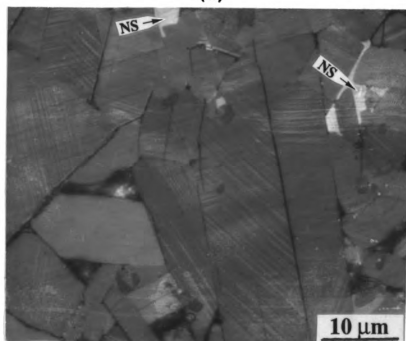


(b)

Fig. 14. Optical microscopy of pure 1:2:3 sample, sintered at 920 C (a) 500x (b) 2000x.



(a)

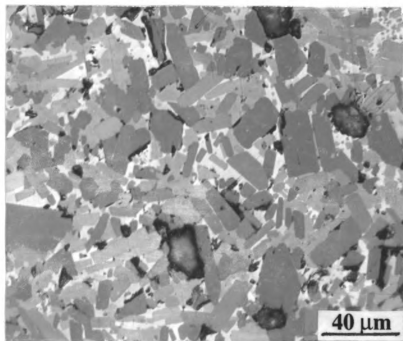


(b)

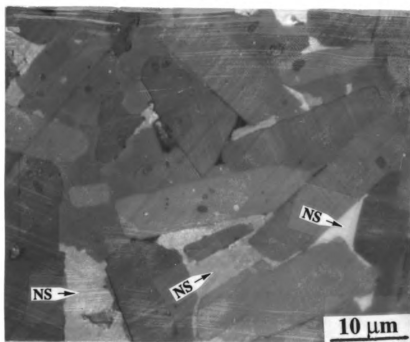
Fig. 15. Optical microscopy of PbO 5 wt% mixed sample, sintered at 920 C (a) 500x (b) 2000x.

Figs 16 and 17 show optical micrographs for 1:2:3 sample mixed with 10 and 15 wt% of PbO, respectively. It can be seen that the amount of non-superconducting phases are further increased as compared to pure 1:2:3 and 1:2:3 mixed with 5 wt% of PbO.

Fig 18 shows the optical micrographs for 1:2:3 mixed with 5 and 10 wt% of Bi sintered at 950 C. It can be seen that the porosity was not improved with the addition of Bi and significant amounts of non-superconducting phases were found even with an addition of 5 wt% Bi.



(a)



(b)

Fig. 16. Optical microscopy of PbO 10 wt% mixed sample, sintered at 920 °C (a) 500x (b) 2000x.

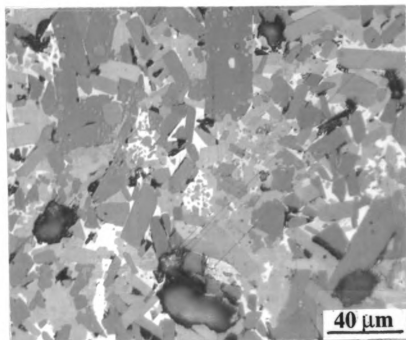
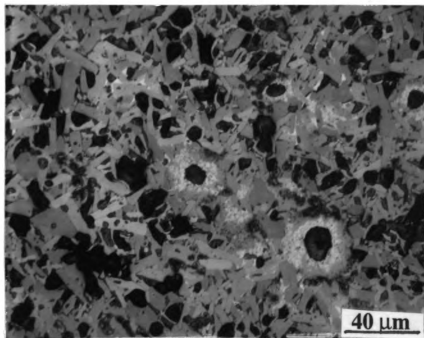
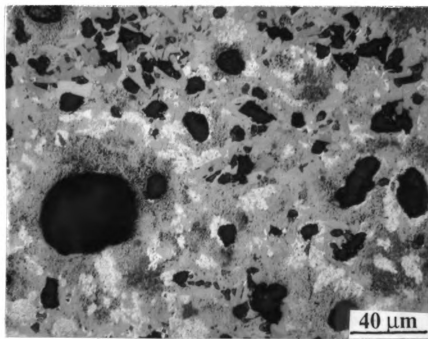


Fig. 17. Optical microscopy of PbO 15 wt% mixed sample, sintered at 920 C (500x).



(a)



(b)

Fig. 18. Optical microscopy of Bi mixed samples, sintered at 950 C (500x) (a) Bi 5 wt% (b) Bi 10wt%.

4-5 Scanning Electron Microscopy and EDAX Analysis

Scanning electron micrographs for reference pure 1:2:3 and PbO mixed samples sintered at 920 C are shown in Fig 19 and Fig 20. It can be seen in Fig 19 that some grains in the PbO 5 wt% mixed sample show well-grown plate-like shape while most of grains in the 1:2:3 sample show rounded shape. In addition to this superconducting phase, a small amount of second phase was also observed in PbO 5 wt% mixed sample, which was identified as Pb-rich non-superconducting phase by EDAX analysis. It can be seen in Fig 20 that the amount of these non-superconducting phase is further increased as the amount of PbO increases. These phases with relatively small grain size and cloud-like shape can be easily distinguished from the plate-like superconducting phase.

Fig 21 shows EDAX spectrum obtained from pure 1:2:3 sample. Data label represent the intensity of elements in terms of counts. From qualitative analysis, no other elements than Y, Ba, Cu were detected. Figs 22 and 23 show EDAX spectrum obtained from PbO 5 and 10 wt% mixed samples, respectively. It can be seen that some additional peaks from Pb were detected in addition to Y, Ba and Cu. The intensity of these peaks increased as the amount of PbO addition increased.

Fig 24 shows EDAX spectrum obtained from the selected grain marked by arrow in Fig 19b, and Figs 25 and 26 show EDAX spectrum obtained from the selected grains marked by

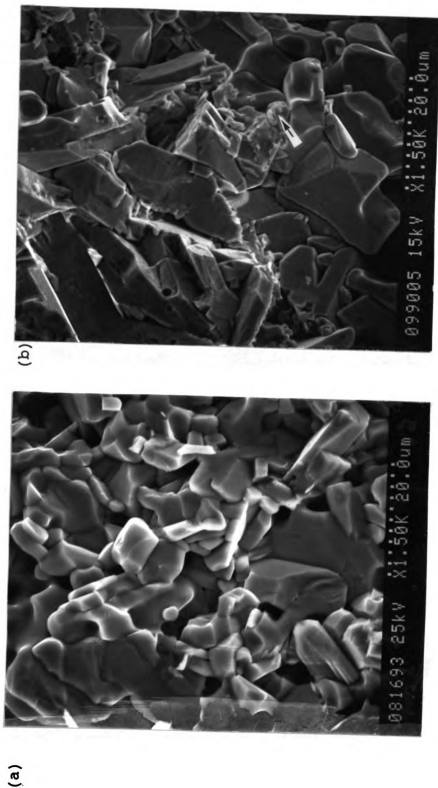


Fig. 19. SEM micrographs of (a) pure 1:2:3 sample (b) PbO 5 wt% mixed sample, sintered at 920 C.

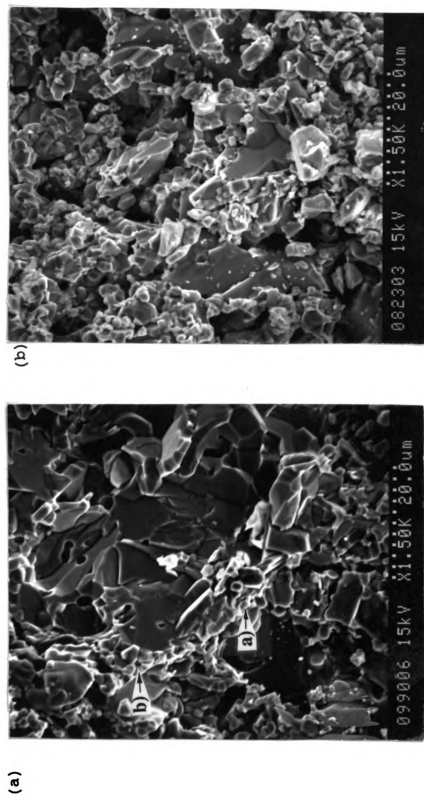
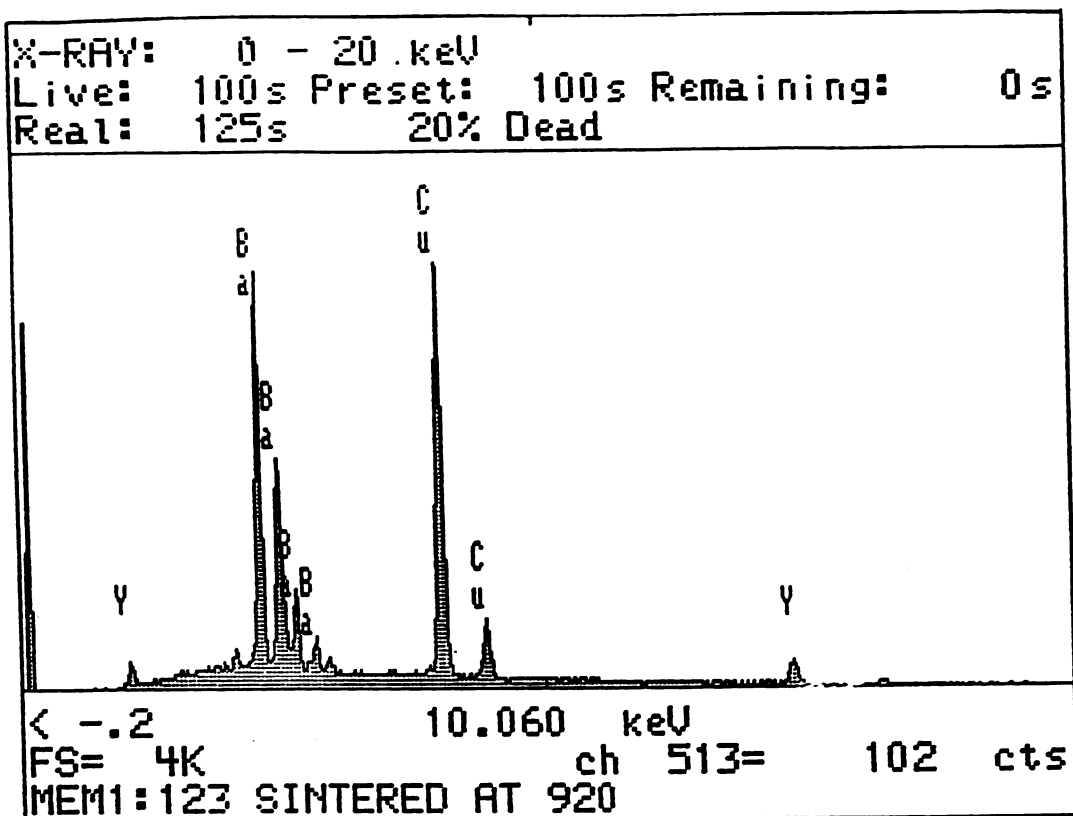
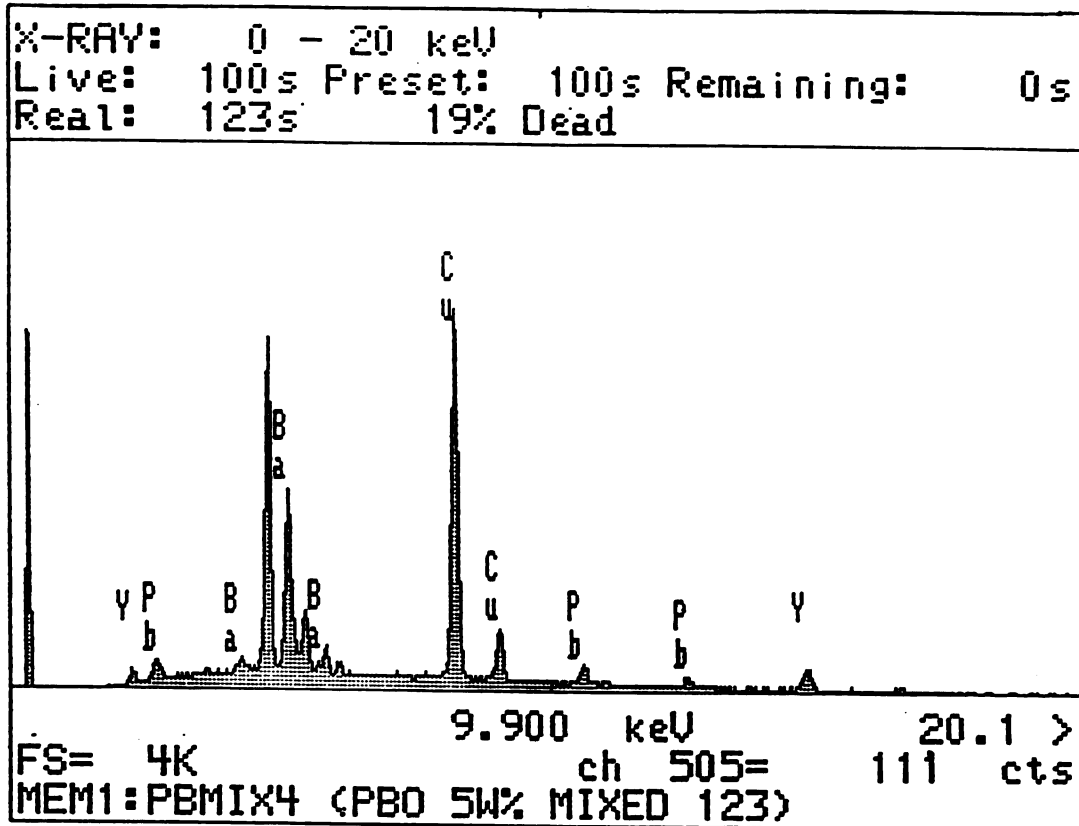


Fig. 20. SEM micrographs of (a) PbO 10 wt% mixed sample
(b) PbO 15 wt% mixed sample, sintered at 920 C.



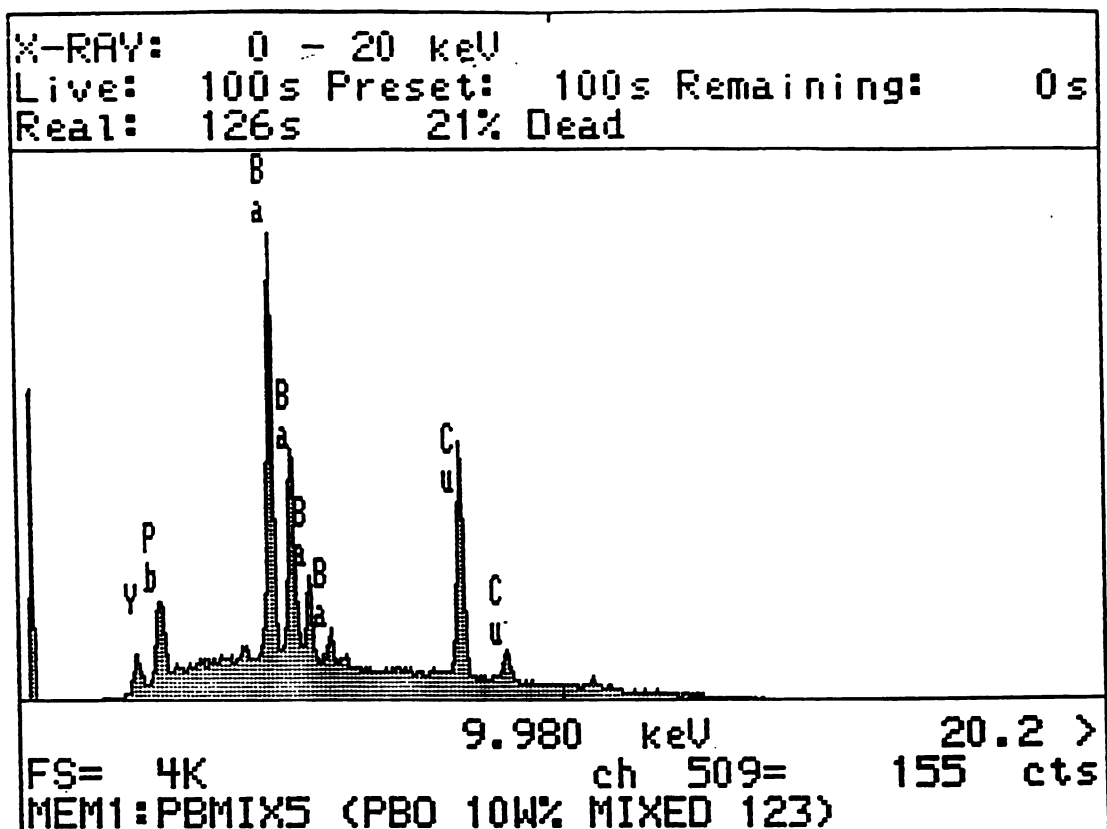
MEM1: WINDOW LABEL	START keV	END keV	WIDTH CHANS	GROSS INTEGRAL	NET INTEGRAL	EFF. FACTOR	%AGE TOTAL
Y	1.82	2.06	13	1825	948	1.00	1.83
BA	4.36	4.58	12	21327	14655	1.00	28.32
BA	4.72	4.98	14	14682	8487	1.00	16.40
BA	5.08	5.26	10	5357	2257	1.00	4.36
BA	5.44	5.62	10	3183	973	1.00	1.88
CU	7.90	8.20	16	25689	21001	1.00	40.59
CU	8.78	9.06	15	5132	2777	1.00	5.37
Y	14.84	15.08	13	2264	646	1.00	1.25

Fig. 21. EDAX spectra obtained from pure 1:2:3 sample, sintered at 920 C.



MEM1: WINDOW LABEL	START keV	END keV	WIDTH CHANS	GROSS INTEGRAL	NET INTEGRAL	EFF. FACTOR	%AGE TOTAL
Y	1.82	2.06	13	1524	582	1.00	1.31
PB	2.24	2.52	15	2535	1003	1.00	2.25
BA	4.36	4.58	12	17764	12322	1.00	27.68
BA	4.72	4.98	14	12433	6910	1.00	15.52
BA	5.08	5.26	10	4719	1629	1.00	3.66
BA	5.44	5.62	10	2749	704	1.00	1.58
CU	7.90	8.20	16	22206	17454	1.00	39.21
CU	8.78	9.06	15	4605	2393	1.00	5.37
PB	10.42	10.66	13	2411	721	1.00	1.62
PB	12.54	12.70	9	1106	188	1.00	.42
Y	14.84	15.08	13	2159	612	1.00	1.37

Fig. 22. EDAX spectra obtained from PbO 5 wt% mixed sample, sintered at 920 C.



MEM1: PB MIX5 (PBO 10W% MIXED 123)

WINDOW LABEL	START keV	END keV	WIDTH CHANS	GROSS INTEGRAL	NET INTEGRAL	EFF. FACTOR	%AGE TOTAL
Y	1.82	2.06	13	3372	1273	1.00	2.62
PB	2.22	2.54	17	8528	4882	1.00	10.06
BA	4.32	4.60	15	25392	18050	1.00	37.21
BA	4.72	4.98	14	16201	8438	1.00	17.39
BA	5.08	5.26	10	6791	2016	1.00	4.16
BA	5.44	5.64	11	4822	1066	1.00	2.20
CU	7.90	8.20	16	16263	11351	1.00	23.40
CU	8.78	9.06	15	4367	1435	1.00	2.96

Fig. 23. EDAX spectra obtained from PbO 10 wt% mixed sample, sintered at 920 C.

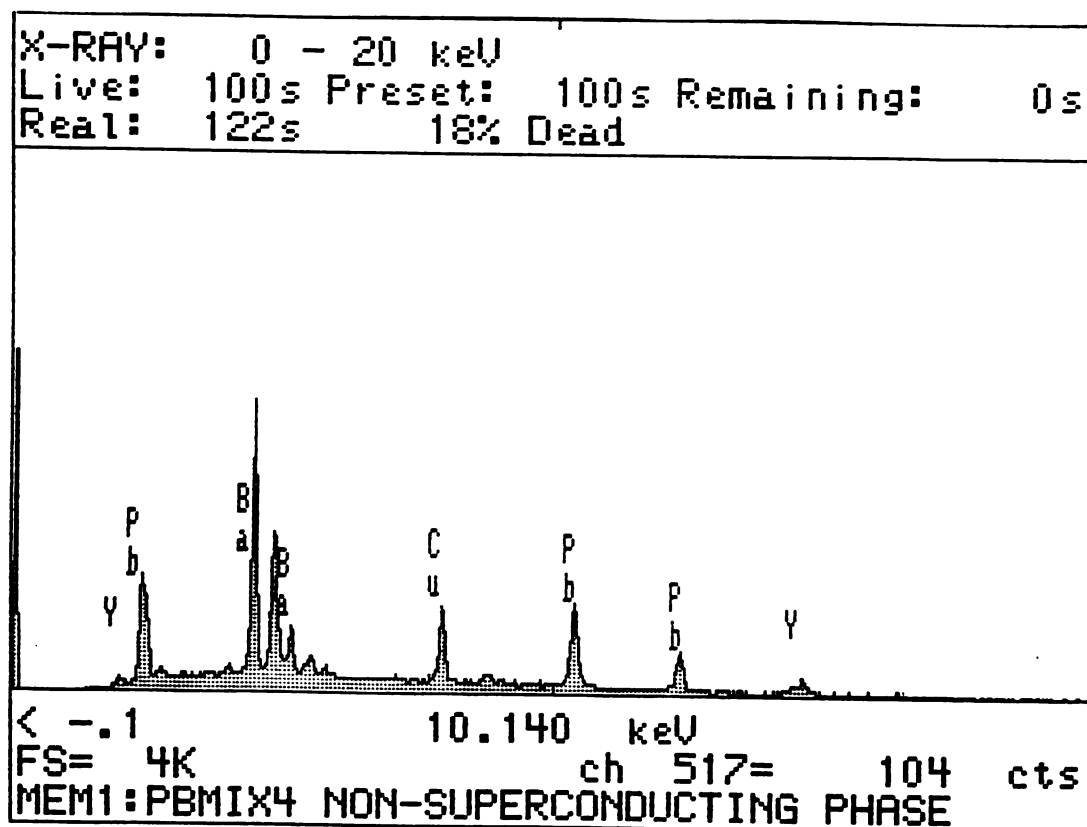


Fig. 24. EDAX spectra obtained from the selected grain marked by arrow in Fig 19b.

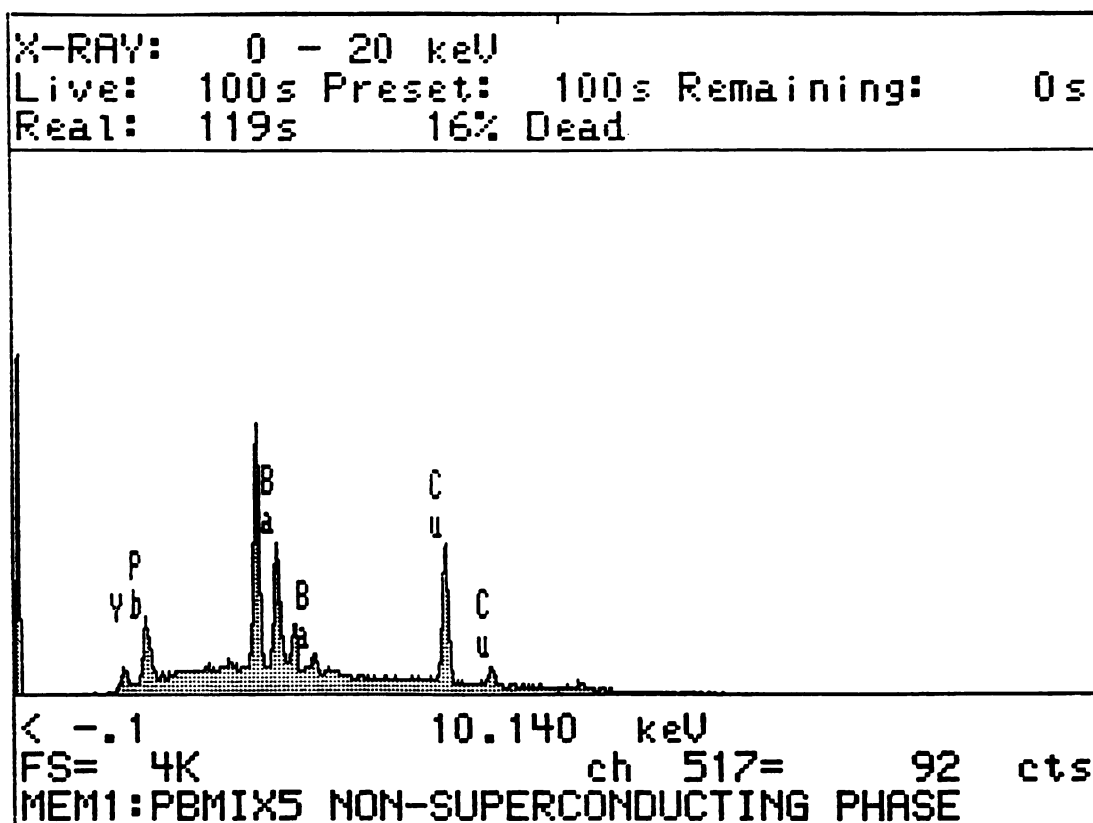


Fig. 25. EDAX spectra obtained from the selected grain marked by a in Fig 20a.

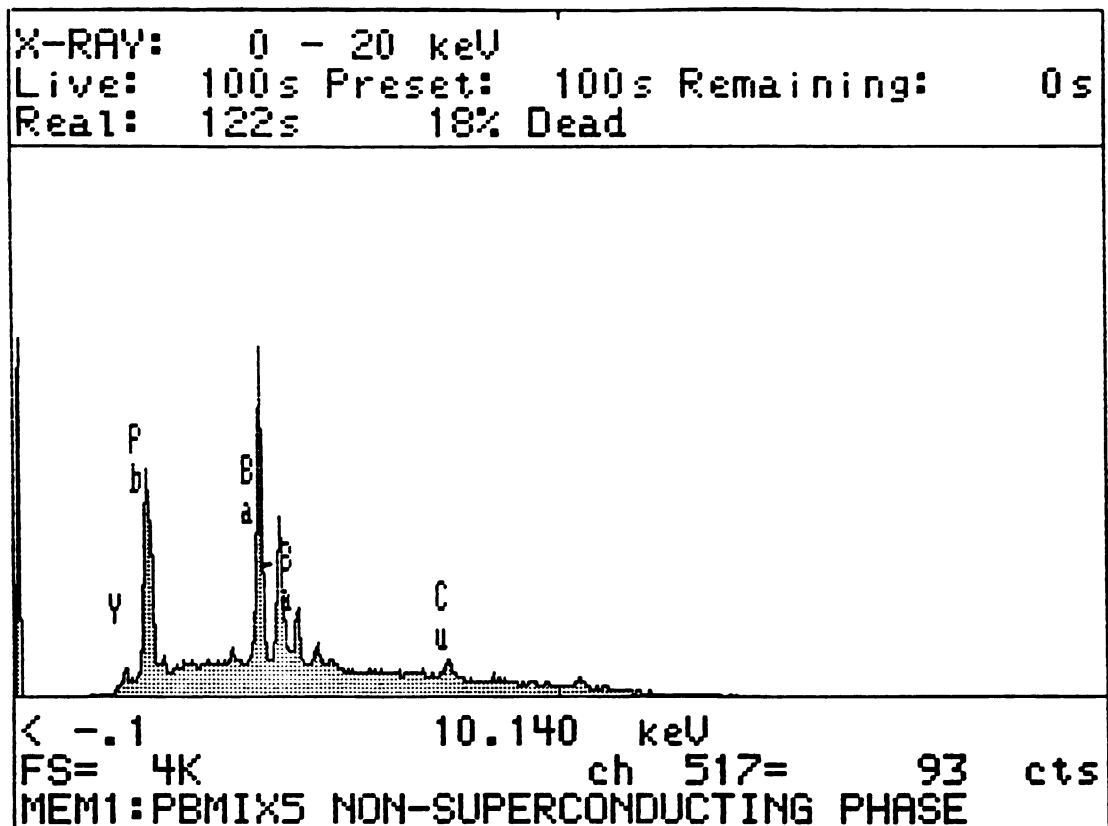


Fig. 26. EDAX spectra obtained from the selected grain marked by b in Fig 20a

'a' and 'b' in Fig 20a respectively. Strong Pb peaks were observed in all of these selected grains while these Pb peaks were not detected in superconducting grains in these samples. Therefore, it is considered that PbO reacts with 1:2:3 superconducting phase, which results in the formation of Pb-rich non-superconducting phase. It can also be seen that while grain marked by 'a' in Fig 20a contains all of Y, Ba, Cu and Pb, grain marked by 'b' is extremely rich in Pb with a very small amount of Cu. Thus, it can be assumed that non-superconducting phases resulted from the reaction between 1:2:3 and PbO do not have homogeneous chemical composition.

5. SUMMARY

In this study, the effect of Bi and PbO addition in the Y-Ba-Cu-O compound on reduction in porosity and the superconducting properties was investigated. Bi and PbO were selected as additives with an objective to employ liquid phase sintering. Followings are the main conclusions of this study:

1. Bi addition in the Y-Ba-Cu-O compound does not reduce the porosity and the x-ray diffraction data shows that even 5 wt% of Bi addition produced a considerable amount of non-superconducting phases which resulted from the reaction between Bi and 1:2:3 compound.

2. On the contrary, 5 wt% of PbO addition in Y-Ba-Cu-O compound reduces the porosity by 7 to 8% without affecting the transition temperature. EDAX analysis however shows that PbO also reacts with 1:2:3 compound and forms a negligible amount of Pb-rich non-superconducting phases.

3. While this improvement in porosity is expected to enhance the mechanical properties, the formation of non-superconducting phases might affect the critical current density by separating superconducting grains. Therefore, to observe the possibility of using PbO as a sintering aid, some supplemental experiments such as critical current density and mechanical test should be carried out.

6. REFERENCES

1. M.K. Wu, J.R. Ashburn and C.W. Chu, Phys. Rev. Lett., Vol. 58, 908 (1987)
2. S. Feng, X. Zhu, C. Lin, C. Wei, Z. Liu, Y. Sun, K. Wu, Z. Shen, J. Li and Z. Gan, International Journal of Modern Physics B, Vol. 1, No 2, 425 (1987)
3. M.F. Yan, W.W. Rhodes and P.K. Gallagher, J. Appl. Phys., Vol. 63 (3), 821 (1988)
4. W. Murphy, S. Sunshine, R.B. Dover, R.J. Cava, B. Batlogg, S.M. Zahurak and L.F. Scheemeyer, Phys. Rev. Lett., Vol. 58., 1888 (1987)
5. G. Xiao, F.H. Streitz, A. Gavrin, Y.W. Du and C.L. Chien, Phys. Rev. B, Vol. 35, 8782 (1987)
6. Y. Maeno, T. Tomita, M. Kyogoku, S. Awaji, Y. Aoki, K. Hoshino, A. Minami and T. Fujita, Nature, Vol. 328, 512 (1987)
7. S.X. Dou, N. Savvides, X.Y. Sun, A.J. Bourdillon, C.C. Sorrell, J.P. Zhou and K.E. Easterling, J. Phys. C: Solid State Phys., Vol. 20, L1003 (1987)
8. R.J.O Jarvinen, K.J. Niemi, T.A. Mantila, E.S. Heikkila and P.T. Vuorinen, Physica C, Vol. 153-155, 882 (1988)
9. L.B. Harris, F.K. Nyang, J. Mat. Sci. Lett, Vol. 7, 801 (1988)
10. K. Takaki, K. Miauchi, Y. Ito, T. Aida, H. Hasegawa and U. Kawabe, Jpn. J. Appl. Phys., Vol. 26, L699 (1987)
11. K. Samananda, A.K. Singh, M.A. Iman, M. Osofsky, V.L. Tourneau and L.E. Richards, Advanced Ceramic Materials, Vol. 3 (5), 524 (1988)
12. S. Jin, T.H. Tiefel, R.C. Sherwood, G.W. Kammlott and S.M. Zahurak, Appl. Phys. Lett., Vol. 51 (12), 943 (1987)
13. N. Kawahara, H. Enami, Y. Kitoh, T. Shinohara, S. Kawabata, H. Hoshizaki, A. Matsumuro and T. Imura, Jpn. J. Appl. Phys, Vol. 28, No. 4, 615 (1989)
14. Y. Fuchang, C. Shoutian, L. Jianmin, L.Fuyi, S. Hongtao, W. Xiaoqing, Y. Baitun and Y. Xi, International Journal of Modern Physics B, Vol. 1, No 2, 209 (1987)
15. J.M. Tarascon, L.H. Greene, P. Barboux, W.R. Mckinnon and G.W. Hull, Phys. Rev. B, Vol. 36, 8393 (1987)
16. F. Mizuno, H. Masuda, I. Hirabayashi and S. Tanaka, Jpn. J. Appl. Phys., Vol. 28, No. 5, L780 (1988)

17. D. PAVUNA, H. Berger, J.L. Tholence, M. Affronte,
A. Dubas, P. Bugnon and F. Vasey, Physica C, Vol.
153-155, 1339 (1988)
18. V. Plechacek, V. Landa, Z. Blazek, J. Sneider,
Z. TrezBalova and M. Cermak, Physica C, Vol. 153-155,
878 (1988)
19. H. Kumakuru, M. Uehara, K. Takahashi and K. Togano,
Physica C, Vol. 153-155, 363 (1988)
20. J.K. Tien, J.C. Borofka, B.C. Hendrix, T. Caulfield and
S.H. Reichman, Metallurgical Transactions A, Vol. 19,
1841 (1988)
21. S. Jin, T.H. Tiefel, R.C. Sherwood, R.B. Dover,
M.E. Davis, G.W. Kammlott and R.A. Fastnacht, Phys.
Rev. B, Vol. 37, 7850 (1988)
22. S. Jin, T.H. Tiefel, R.C. Sherwood, R.B. Dover,
M.E. Davis, G.W. Kammlott and R.A. Fastnacht, Appl.
Phys. Lett., Vol. 52 (24) 2074 (1988)
23. "Omega complete temp. measurement handbook and
encyclopedia", T-45 (1987)
24. "A.S.T.M Standard", B 328-73 (1987)
25. Y. Syono, M. Kikuchi, K. Ohishi, K. Hiraga, H. Arai, Y.
Matsui, N. Kobayashi, T. Sasaoka and Y. Muto, Jpn. J.
Appl. Phys. Vol. 26, L498 (1987)
26. N.D. Patel, P. Sarkar, T. Troczynski, A. Tan and P.S.
Nicholson, Adv. Ceramic Materials, Vol. 2, 615 (1987)
27. C.S. Pande, A.K. Singh and A. DasGupta, J. Met., Jan.,
10 (1988)

MICHIGAN STATE UNIV. LIBRARIES



31293009175526